Adsorption And Stabilization Studies Of Polymers On Latex Particles.

Ahmed, Maqsood Syed

ADSORPTION AND STABILIZATION STUDIES OF POLYMERS ON LATEX PARTICLES

Lehigh University PH.D. 1984

ADSORPTION AND STABILIZATION STUDIES OF POLYMERS ON LATEX PARTICLES

BY

MAQSOOD SYED AHMED

A DISSERTATION

PRESENTED TO THE GRADUATE COMMITTEE

OF LEHIGH UNIVERSITY

IN CANDIDACY FOR THE DEGREE OF

DOCTOR OF PHILOSOPHY

IN

POLYMER SCIENCE AND ENGINEERING

LEHIGH UNIVERSITY

1984

CERTIFICATE OF APPROVAL

Approved and recommended for acceptance as a dissertation in partial fulfillment of the requirements for the degree of Doctor of Philosophy.

September 21, 1984
(date)

John W. Vanderhoff
(Professor in Charge)

John W. Vanderhoff
Accepted

Special committee directing the doctoral work of Mr. Maqsood Ahmed

John W. Vanderhoff
John W. Vanderhoff, Chairman

Mohamed S. El-Aasser, Co-advisor

Frederick M. Fowkes

Wiley E. Daniels

Andrew Klein

DEDICATION

To all my educators, especially my parents.

ACKNOWLEDGMENTS

It is my pleasure to thank my Professors, Dr. M. S. El-Aasser and Dr. J. W. Vanderhoff, for their advice on the subject matter of this work.

Sincere thanks are extended to Dr. F. M. Fowkes for his deep interest, helpful discussions, and encouragement throughout this study.

Thanks are also extended to Dr. A. Klein and Dr. W. E. Daniels for their interest and for serving on the dissertation committee; Dr. D. Nagy (Air Products and Chemicals, Inc.) for his assistance with photon correlation spectroscopy measurements; Mr. S. Knochs (Bethlehem Steel Corporation) for his help and kindness during calorimetric measurements.

Thanks are also extended to my colleagues, especially David, and other staff members, for their assistance and cooperation; Mrs. K. Devlin for typing the manuscript; the Emulsion Polymers Institute and the Emulsion Polymers Liaison Program for the financial support during this work.

Finally, I am greatful to my parents, sisters, and brothers, without their love and encouragement this work would not have been possible.

TABLE OF CONTENTS

TABLE OF CONTENTS (Contd.)

TABLE OF CONTENTS (Contd.)

TABLE OF CONTENTS (Contd.)

LIST OF TABLES

LIST OF TABLES (contd.)

LIST OF FIGURES

LIST OF FIGURES (Contd.)

LIST OF FIGURES (Contd.)

ABSTRACT

Polymer adsorption is important in the stabilization or flocculation of colloidal sols. The adsorption of polyvinyl alcohol (PVA) was studied because of its practical application in textiles, adhesives, and coatings. The solution properties of polyvinyl alcohol were investigated to determine the conformation of the polymer coil (which affects the adsorption) using: a) differential refractometry; b) viscometry; c) electron microscopy; d) gel permeation chromatography. No evidence of association of the polyvinyl alcohol molecules in dilute solution was found with either the fully hydrolyzed or the partially hydrolyzed (88%) polyvinyl alcohols; however, concentrated (>10%) solutions of the fully hydrolyzed polyvinyl alcohol gave gel permeation chromatograms with a shoulder or a distinct second peak.

The adsorption of polyvinyl alcohol on monodisperse polystyrene latex particles was investigated, specifically, the effect of molecular weight and degree of hydrolysis of the polyvinyl alcohol on the adsorption density, adsorbed layer thickness, and heat of adsorption. The adsorption isotherms, determined using the serum replacement adsorption and desorption methods, showed an initial rapid rise in surface concentration, followed by a gradual increase to an apparent plateau. Extension of the adsorption isotherms

to higher concentrations gave a second rise in surface concentration, which was attributed to multilayer adsorption and incipient phase separation at the interface. The desorption isotherms comprised two regions: a region of decreasing surface concentration, indicating that the adsorption of the polymer in multilayers is reversible, followed by a region of constant surface concentration, indicating that the adsorption of the polymer in the monolayer is irreversible. The adsorption densities at the apparent plateau followed the relationship $\Gamma \alpha M^{0.5}$ for the fully hydrolyzed polyvinyl alcohol and $\Gamma \alpha M^{0.72}$ for the 88%-hydrolyzed polyvinyl alcohol. The same dependence was found for the adsorbed layer thickness measured by viscosity and photon correlation spectroscopy.

The heats of adsorption were measured using the Tronac Model 1250 Isothermal Microcalorimeter. The evolution of heat during adsorption was found to be slow. For polyvinyl alcohols of different molecular weights and degrees of hydrolysis adsorbed on 190nm-size monodisperse polystyrene latex particles, the equilibrium heats of adsorption were attained only after 800 minutes. The heats of adsorption increased with increasing molecular weight and decreasing degree of hydrolysis, and were 25-95 times greater than expected from mere hydrophobic interactions with the surface. The higher heats of adsorption were attributed to increased polymer-solvent interactions in the

adsorbed layer.

The effect of polystyrene latex particle size on the adsorption density, adsorbed layer thickness, and heat of adsorption was also investigated using particle sizes of 190, 400, and 1100nm. The shape of the adsorption isotherm and the adsorption density were found to be independent of the latex particle size, yet the thickness of the adsorbed layer increased with increasing particle size. The increase in thickness of the adsorbed layer followed the relationship $\delta \alpha R^{0.5}$ over the 190-1100nm particle size range. The effect of increasing particle size on the heat of adsorption was to decrease the heats of adsorption and shorten the time required to attain equilibrium. This was explained in terms of the different configurations of the polyvinyl alcohol molecules adsorbed on surfaces of different curvature and the slow diffusion process of adsorption governed by dispersion forces.

The effect of adsorbed polyvinyl alcohol on the colloidal stability of the 190nm and 400nm diameter polystyrene particles was measured by determining the critical coagulation (flocculation) concentrations with sodium chloride. The critical coagulation concentrations showed that the bare particles coagulated in the primary minimum and the critical flocculation concentrations showed that polyvinyl alcohol-covered particles flocculated in the

secondary minimum; in both cases, the larger particles were less stable than the smaller particles. Electrophoretic mobility measurements as a function of electrolyte concentration corroborated the electrolyte stability measurements. The compression of the latexes in a serum replacement cell showed that the maximum volume fraction of the volume fraction-pressure curve was greater for the polyvinyl alcohol-covered particles than for the bare particles, but that there was no difference between the different-size particles.

1. INTRODUCTION

1.1 Polymer Adsorption

Polymer adsorption is important in many industries. Eirich (1) has listed its many applications in such diverse industries as agriculture, pharmaceutical, paper, paint, and water treatment, and several recent reviews (2-6) have described the significant advances made over the past three decades in the theoretical treatment of the mechanism of polymer adsorption.

The adsorption of a polymer molecule at a liquid-solid interface is complicated. Unlike low-molecular-weight emulsifiers, which adsorb in a monolayer in which each emulsifier molecule orients itself vertically, with a single contact point at the interface, the polymer coil forms multiple contacts, with the intervening segments extending into the liquid phase (Figure 1.1). This model was proposed in 1951 by Jenkel and Rumbach (7), who found that the amount of polymer adsorbed per unit surface area corresponded to a layer more than 10 molecules thick if all the segments of the polymer chain were attached to the surface. This led to the loop-train model of polymer adsorption, which is now widely accepted. Those segments in direct contact with the surface are the trains and those intervening segments extending into the liquid phase are the loops; each polymer molecule has two

ends (the tails), which also extend into the liquid phase.

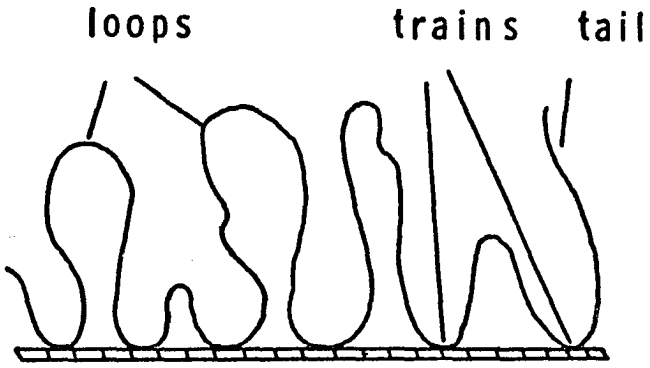

Figure 1.1. Schematic Representation of Loop-Train Model.

A complete characterization of the adsorption behavior of a polymer comprises the determination of five parameters: (i) the adsorption density (Γ); (ii) the thickness of the adsorbed layer (δ); (iii) the heat of adsorption (ΔH_{ads}); (iv) the fraction of polymer bound to the surface (p); (v) the segmental density distribution ($\rho(z)$). The adsorption density (unit weight of adsorbate per unit surface area at saturation adsorption) is the parameter most commonly reported because it is easily determined from the adsorption isotherm, which is obtained from the mass balance of the added polymer. The thickness of the adsorbed layer is measured optically by ellipsometry or hydrodynamically by viscometry, ultracentrifugation, or light scattering. The optical method depends on the differences in refractive in-

dices of the adsorbent, adsorbate, and bulk liquid phase; it also requires a flat, reflecting surface, which makes it impractical for colloidal particles. The heat of adsorption is determined from: (i) the temperature dependence of the adsorption isotherm determined using the Clausius-Clapeyron relation, which assumes isostericity and reversibility of adsorption, conditions not fulfilled in polymer adsorption (8); (ii) direct calorimetric measurements, which are usually used. The fraction of polymer bound to the surface is measured directly by spectroscopic techniques such as infrared (IR), nuclear magnetic resonance (NMR), or electron spin resonance (ESR) spectroscopy, and indirectly by microcalorimetry. The IR method depends upon the spectral shifts of functional groups upon adsorption (9,10). The NMR and ESR methods depend upon the different mobilities of the segments in the trains and loops. Microcalorimetry has been used (8) to measure the bound polymer fraction; however, it requires a comparison of the heat of adsorption of the polymer molecule with that of a small molecule of structure equivalent to that of a polymer segment, a condition which is not easily met. The segment density distribution is the most difficult parameter to measure experimentally; in the past, its determination has been limited to theoretical derivations; however, this distribution was measured recently by small-angle nuetron scattering (11), which offers promise of accurate mea-

surements in the future.

1.1.1 Theories of Polymer Adsorption

Many other theories of polymer adsorption have been proposed since the original loop-train model of Jenkel and Rumbach (7). All of these theories depend upon the theories of adsorption of small molecules and the principles governing polymer solutions. Statistical thermodynamics was used to formulate and maximize the partition function from which all other thermodynamic functions are calculated. The main differences between these theories are in the partition function models and the mathematical approximations used in the calculation of the results. The following sections describe the Frisch-Simha-Eirich, Silberberg, Hoeve, and Scheutjens-Fleer theories.

1.1.1.1 Frisch-Simha-Eirich Theory (12-16). This is the earliest theory based on the random-walk concept and formulated in terms of a diffusion equation. A lattice model was used for the surface and bulk solution, and the polymer was represented by a random-walk configuration on the lattice. The interface was treated as a reflecting barrier, so that the probabilities of performing steps in all directions except toward the interface were equal. The derived expression for the adsorption isotherm was:

$$\frac{\theta}{1-\theta} \exp(2K_1\theta) = (Kc)^{1/\langle v \rangle} \qquad 1.1$$

where θ is the surface coverage, c the polymer concentration

in the bulk solution, k_1 and k the constants, and <v> the average number of segments in contact with the surface. Values of <v> of unity give Langmuir-type isotherms; values greater than unity give high-affinity isotherms. This theory predicts that: (i) increasing the polymer molecular weight gives a higher adsorption density and longer loops; (ii) the number of attached segments per chain is proportional to the square root of the total number of segments. The disadvantages of this theory are that it overestimates the number of different chain conformations and neglects the tails and excluded volume effects.

1.1.1.2 Silberberg Theory (17-21). This theory used a quasi-crystalline lattice model and separate treatments for the segments in the trains and in the loops. The segments in the trains were described by an internal partition function determined from the attractive forces between the segments and the surface; the segments in the loops were described with a different internal partition function, similar to that of the segments in the bulk. Later, the interactions from the segment-segment, segment-solvent, and solvent-solvent contacts were included (19-21). This theory does not give an analytical expression for the adsorption isotherm. Instead, numerical solutions were obtained for the two special cases of athermal and theta solvents. This theory predicts that: (i) for theta conditions, the adsorption density is proportional to the square root of the molecular weight, up to a limiting

molecular weight; (ii) for athermal conditions, the adsorption density varies only slightly with molecular weight; (iii) the loops are small and depend upon the nature of surface and the polymer, but are independent of molecular weight; (iv) the segment density follows a step function, i.e., it is constant between the surface and a distance equal to one-half the loop size and then decreases discontinuously with increasing distance. The disadvantages of this theory are that it assumes only uniform small-size molecular-weight-independent loops and neglects the tail effects.

1.1.1.3 Hoeve Theory (22-26). Instead of the lattice model, this theory used a flexibility parameter C, which can be estimated from the lattice model. The partition functions were derived for the trains and loops (Gaussian distribution) of an isolated polymer chain with any orientation in space. This theory gives an analytical expression for the adsorption isotherm:

$$N_a/S\delta = (N_f/V)\ \exp(-\lambda n) \qquad 1.2$$

where N_a and N_f are the adsorbed and unadsorbed polymer, respectively, S the adsorbing surface area, δ the thickness of the train layer, V is the volume of the bulk solution, λ a function of the adsorption energy, and n the number of polymer segments in a chain. An expression for the segmental distribution $\rho(z)$ in a loop was also derived:

$$\rho(z) = 4\pi^{\frac{1}{2}}\beta_1 c\ \exp\left[-4\beta_1 z(-\lambda)^{\frac{1}{2}}\right]\left[1+S_{-1/2}+S_{-3/2}\right]^{-1} \qquad 1.3$$

where $\beta_1 = 3n/2$ and $\langle r_o^2 \rangle$ is the unperturbed mean square end-to-end distance of the chain with n segments. Equation 1.3 is valid for values of z larger than δ, and states that $\rho(z)$ is a simple exponential function of z. This theory also took into account the solvent and excluded volume effects, which lead to a decrease in the number of possible conformations of the adsorbed polymer chains. An expression for the adsorption isotherm was also derived, which reflects these effects:

$$N_a/S\delta = (N_f/V) \exp\left\{-n\left[\lambda+\tfrac{1}{2}(\tfrac{1}{2}-\chi)KV_2(o)\right]\right\} \qquad 1.4$$

where χ is the interaction parameter. Equation 1.4 reduces to Equation 1.2 when $\chi = 0.5$, i.e., under theta conditions. This theory predicts that: (i) the ability to form loops depends upon the flexibility of the polymer, and the loop size is determined by the free energy of adsorption; (ii) adsorption from athermal solvent gives smaller loops and longer trains; (iii) adsorption from theta solvent gives longer loops and short trains; (iv) the adsorption density and the adsorbed layer thickness are proportional to the square root of the molecular weight for long chains under theta conditions; (v) the segment density profile is an exponential function. The disadvantage of this theory is that it neglects the tail effects.

1.1.1.4 Scheutjens-Fleer Theory (27-28). This theory used a lattice model and defined the conformation of the adsorbed

chain by the layer number in which a specified segment is found; the partition functions were then written for a specified set of conformations. The partition function comprises contributions from the polymer-solvent interaction in each layer and the adsorption energy in the first layer. All possible conformations of the loops-trains and tails were taken into account. The equations were derived by maximizing the partition function, followed by a matrix formalism, and then solved numerically under the boundary constraints for the various adsorption parameters. This is the most comprehensive theory on polymer adsorption developed to date. It does not contradict any of the predictions of the earlier theories. For the adsorption density, it defines two relations based on the polymer chain length r: (i) for small chain lengths ($20<r<1000$) in theta solvent, it predicts that the increase in adsorption density is proportional to the logarithm of the chain length; in a better solvent, the chain length dependence is smaller; (ii) for longer chains in theta solvent, it predicts that the increase in adsorption density is proportional to the square root of the chain length. The thickness of the adsorbed layer is predicted to increase linearly with the square root of the chain length in a theta solvent; the increase is smaller and nonlinear in an athermal solvent. Unlike the earlier theories, this theory does not make an a priori assumption about the segment density profile; the effect of the tails is predicted to be signifi-

cant, and the concentration of loop segments is predicted to decrease exponentially near the surface; however, at greater distances from the surface, the exponential decay is disrupted owing to the dominant effect of the tail segments.

1.1.2 Factors Influencing Polymer Adsorption

A polymer coil in solution has a high degree of conformational freedom, which can be described by random-flight statistics. When the polymer coil adsorbs onto a solid surface, it loses one degree of freedom in the transition from a three-dimensional to a two-dimensional coil. The driving force for adsorption is the decrease in the free energy of the system. If the polymer coil loses entropy on adsorption, the enthalpic contribution to the free energy must be relatively great for adsorption to take place. The enthalpic contribution arises from the binding of the train segments to the surface, which involves the breaking of solvent-surface bonds and the formation of segment-surface bonds. This process is affected by several factors, e.g., the state of the free polymer coil in solution and the parameters governing the adsorption at the liquid-solid interface. These factors are classified and discussed briefly in the following sections.

a) Structural Variations. This category includes the effects of the molecular weight, molecular weight distribution, degree of branching, blockiness, and flexibility of the polymer chain. Increasing the polymer molecular weight gives

high affinity-type isotherms, high adsorption densities, thicker adsorbed films, and lower bound polymer fractions. The exact magnitude of these effects depends upon the nature of the solvent. For a theta solvent, $\Gamma \alpha M^{0.5}$, $\delta \alpha M^{0.5}$, and $p \alpha 1/M$. For an athermal solvent, the effects are weaker. The molecular weight distribution affects the shape of the isotherm; samples of narrow molecular weight distribution give isotherms with sharp inflection points; samples of broad molecular weight distribution give rounded inflection points. The degree of branching has no effect on the shape of the adsorption isotherm; however, the adsorption density of a branched polymer is larger and the adsorbed layer thickness is slightly smaller than that of a linear polymer of the same molecular weight (3). Block copolymers are more surface-active because the different segments of the chain have different affinities for the solvent and the surface; therefore, higher adsorption densities are expected. The flexibility of the chain affects the formation of the loops and their size; however, systematic investigations of this parameter have not yet been carried out.

b) Concentration Variations. The concentration of the polymer solution affects the adsorption isotherms. At very low polymer concentrations, the polymer chains are dispersed individually. The measurement of adsorption from such dilute solutions is often difficult, for two reasons: (i) the initial rise in surface concentration is rapid; (ii) it is

difficult to measure such low concentrations accurately. With increasing polymer concentration, the interactions between the polymer molecules become important. At low surface concentrations, the polymer molecules assume a flatter configuration, which rearranges with increasing surface concentration; the values of the bound-polymer fraction decrease from high to low values with increasing surface concentration. At still higher polymer concentrations, the polymer chains overlap to give multilayer adsorption.

c) Interaction Parameters. This category includes the polymer-surface, polymer-solvent, polymer-polymer, and solvent-surface interactions, all of which affect the adsorption. Polymer-surface interactions determine the adsorption energy, which in turn determines the loop size; for large adsorption energies, the trains are longer and the loops are relatively small; conversely, for small adsorption energies, the loops are larger. Polymer-solvent interactions have a drastic effect on the adsorption; generally, adsorption from a good solvent gives lower adsorption densities and adsorbed layer thicknesses than adsorption from a theta solvent. Polymer-polymer interactions in the adsorbed layer become significant at high surface concentrations and can lead to a further decrease in the free energy of adsorption. Solvent-surface interactions generally are negligible for hydrophobic surfaces in aqueous media and therefore have little effect on adsorption.

d) Other Variations. Time and temperature are the other important parameters which affect adsorption. Polymer molecules require longer times to attain adsorption equilibrium; therefore, care must be taken that sufficient time is allowed for the adsorption to reach equilibrium. Temperature affects the mobility of the polymer molecules and the solvent power. The temperature coefficient of adsorption of a given polymer varies according to the nature of the solvent and the surface (29), which can lead to an increase or decrease in the adsorption density with temperature; therefore, no general conclusions can be drawn. The effects of temperature are much greater in nonaqueous than in aqueous systems.

1.2 Stabilization by Polymer Adsorption

The effect of polymer adsorption on colloidal stabilization was known even to the ancient people, who used such natural materials as glue, gum arabic, and rosin to prepare stable dispersions, but it was only very recently that the mechanism of this process has been established. The term "steric stabilization" was introduced in 1954 by Heller and Pugh (30) to explain the stabilization of colloidal sols by adsorbed uncharged polymer molecules. This terminology has been used imprecisely until recently, when three types of polymeric stabilization were postulated: (i) steric stabilization, in which the uncharged polymer molecules stabilizing the colloidal particles are adsorbed on the particles;

(ii) depletion stabilization, in which the polymer molecules stabilizing the colloidal particles are free in solution; (iii) electrosteric stabilization (a combination of electrostatic and steric stabilization), in which the particles are charged or the polymer is a polyelectrolyte.

Steric or electrosteric stabilization are widely used in practical systems because of their advantages over electrostatic stabilization. Colloidal dispersions stabilized sterically or electrosterically are stable to the addition of electrolyte. Steric stabilization is effective in nonaqueous systems where electrostatic stabilization is ineffective; moreover, it is effective at both high and low volume fractions of dispersed phase and thus is useful for the preparation of high-solids dispersions.

The stabilization of colloidal particles is the result of the various attractive and repulsive interparticle forces. The following sections describe these forces in detail, except for depletion stabilization, which is not effective in these systems and therefore is omitted.

1.2.1 Van der Waals Attraction

The attractive forces operative between two colloidal particles are the Van der Waals or London dispersion forces. These forces arise from the random fluctuations in the electric field of an atom according to the Heisenberg uncertainty principle. These fluctuations result in the formation of a transient dipole or a multipole, which can induce a dipole

or multipole in another atom or molecule.

There are two methods to calculate the magnitude of the Van der Waals attraction between colloidal particles in a dispersion: (i) the Hamaker microscopic approach (31); (ii) the Lifshitz macroscopic approach (32). In the classicial Hamaker microscopic approach, the interactions between two macroscopic bodies are obtained by summing pairwise the interactions between individual constituent atoms or molecules, especially those occurring at the ultraviolet frequencies. In contrast, in the Lifshitz macroscopic approach, the interactions are calculated directly from the measured dielectric properties of the macroscopic bodies over the entire frequency spectrum. This latter approach is superior to the Hamaker approach in that it allows for all many-body interactions, permits inclusion of all frequencies of interactions, and properly accounts for the presence of a third medium between the bodies.

The presence of an adsorbed layer of Hamaker constant different from that of the particle alters the attractive forces between the particles. Vold (33) and Vincent (34) have shown that the attraction between particles with an adsorbed layer may increase or decrease depending upon the composition of the adsorbed layer. Generally, however, the effect of the adsorbed layer on the magnitude of the attractive forces is small and thus can be neglected.

1.2.2 Electrostatic Repulsion

Colloidal particles with charges of the same sign repel one another by electrostatic repulsion; however, electroneutrality requires that the net charge of the particles and their immediate surroundings be zero, i.e., if the particle surface is charged, there must be an equivalent countercharge, which together with the surface charge constitutes the electric double layer. The countercharges are distributed diffusively, their concentration decreasing rapidly with increasing distance from the particle surface. When the two particles approach one another, their electric double layers begin to interpenetrate at significant interparticle distances, leading to electrostatic repulsion.

Any quantitative theory of electrostatic repulsion requires the formulation of the distribution of electric charge or potential around the colloidal particles. Two basic models have been developed to describe the charge distribution around a colloidal particle: (i) the diffuse double layer; (ii) the Stern diffuse double layer. Three basic equations, i.e., the Poisson and Boltzmann equations, and the equation for the space charge density, were used to calculate the ion distribution in the diffuse part of the double layer. The analytical solution of these equations is difficult. Gouy and Chapman (35,36) derived an approximate solution of the combined Poisson-Boltzmann equation, which represents the potential in the diffuse part of the double layer. Num-

erous papers have dealt with the limits of application of the Poisson-Boltzmann equation and the assumptions made in the Gouy-Chapman model.

Stern (37), and later Grahame (38), developed a theory which eliminated the discrepancies between the experimental results and the decrease in potential with distance calculated from the Gouy-Chapman model. In the Stern-Grahame model, the counterions are distributed in two layers: (i) the Stern (Helmholtz) layer at distance δ from the particle surface; (ii) the diffuse double layer outside the Stern layer. Stern and Grahame took into account the finite size of the ions and added an absorption-dependent term to the interaction energy in the Boltzmann equation. Two cases were considered in the approach of two charged particles to one another and the consequent overlap of their diffuse double layers: (i) the surface potential remains constant while the charge decreases; (ii) the surface charge remains constant while the potential increases. In both cases, the free energy of the double layer increases upon interaction and hence work must be done to bring the particles closer together, i.e., both cases lead to repulsion. These electrostatic repulsive forces were calculated by Verwey and Overbeek (39), and Derjaguin and Landau (40-43).

The adsorption of a polymer on the surface of a charged particle alters the double layer, and hence the repulsive forces, by the displacement of the counterions and the al-

teration of the dielectric constant of the double layer. Brook (44) investigated the effect of an adsorbed polymer layer on the distribution of counterions. His theoretical calculations showed that the thickness of the double layer increased with the adsorption of polymer, suggesting that the interparticle repulsion begins at longer distances. For the case where the polymer is a polyelectrolyte and thus bears changes, the calculation becomes more complicated.

1.2.3 Steric Repulsion

Steric forces are non-electrostatic repulsive forces. Their existence was recognized from the stabilization of colloidal particles by nonionic polymer molecules in systems where the electrostatic repulsive forces were considered to be nonexistent. When two particles with adsorbed polymer layers approach one another, interpenetration or compression of the polymer coils takes place, leading to a change in the Gibbs free energy (ΔG_R), which is given by:

$$\Delta G_R = \Delta H_R - T\Delta S_R \qquad 1.5$$

For two particles to repel one another, the ΔG_R of interpenetration must be positive. Positive values of ΔG_R can result in three different ways: (i) both the entropic (ΔS_R) and enthalpic (ΔH_R) components of the ΔG_R of interpenetration are negative, but the entropic component outweighs the enthalpic component; (ii) both the entropic and enthalpic components are positive, but the enthalpic component out-

weighs the entropic component; (iii) the entropic component is negative and the enthalpic component is positive, with both components contributing to the stability. Thus steric repulsion may arise from the entropic, enthalpic, or combined enthalpic-entropic effects of the interpenetration of the adsorbed polymer coils.

There are two approaches to quantify steric repulsion forces: (i) classical thermodynamics; (ii) statistical thermodynamics. The classical thermodynamic approach is based on the Gibbs-Helmholtz relation (Equation 1.5), which is independent of any molecular model but provides little information on the source and magnitude of the free energy.

Statistical thermodynamics, which is a powerful approach to calculate the free energy, requires a molecular model. Mackor (45), Mackor and Van der Waals (46), and Clayfield and Lumb (47-50) used different models in which the magnitude of the free energy was based solely on the loss in configurational entropy of polymer molecules on interpenetration, i.e., they were applicable only to media which were poor solvents for the polymer. Fischer (51) considered the effect of solvent properties of the medium to arise from the chemical potential gradient between the solvent in the intersecting zone and the bulk medium; he related the repulsive potential energy to the second virial coefficient of the polymer solution, i.e., a repulsive potential is generated in a medium which is a good solvent for the polymer, but not

in a medium which is a poor solvent. Meier (52) combined the entropic (volume restriction effect) approaches of Mackor, and Clayfield and Lumb, with Fischer's solvency approach (osmotic pressure or mixing effect) to produce a hybrid general theory formulated in terms of the Flory-Huggins theory; he found that the mixing contribution was significant for particles with extensive polymer surface coverage in good solvents. Later, Hesselink, Vrij, and Overbeek (53) corrected and improved Meier's model; they recalculated the loss in configurational entropy of the tails and loops resulting from volume restriction and used the improved segment density distribution function calculated by Hesselink (54-55). Napper et al. (56) pointed out an error in these calculations which arose from the separate calculation of the configurational entropy in the mixing of solvent with compressed polymer, whereas the mixing of solvent should be with randomly coiled uncompressed polymer.

1.2.4 Measurement of Repulsive Forces

Electrostatic repulsive forces can be measured directly using several techniques. Napper (57) classified the measurement of electrostatic repulsive forces into two categories: (i) equilibrium measurements; (ii) kinetic measurements. The equilibrium measurements are used more frequently. Tabor and Robert (58,59) formed a liquid film between a soft optically-smooth rubber hemisphere and a flat glass surface and measured the liquid film thickness optically

under applied pressure for different electrolyte concentrations; the equilibrium film thickness was determined primarily by double layer repulsion since the Van der Waals attraction was small compared with the applied pressure. Ottewill et al. (60,61) used the osmotic or disjoining pressure of the system to measure the repulsive forces; the colloidal dispersion was confined in a cell with a semipermeable membrane which retained the colloidal particles, and the medium was forced out through the membrane by hydrostatic pressure so that the interparticle spacing decreased, to give the variation of volume fraction of dispersed phase with applied pressure; the magnitude of this pressure was a measure of the repulsive forces. El-Aasser and Robertson (62, 63) used ultracentrifugation to separate the charged particles of the colloidal dispersion into layers, which were forced together against the double layer repulsion; the force between the particles in adjacent layers at a given centrifugal force was calculated for the different particle layers.

There are few direct experimental methods to measure the steric repulsive forces. Doroszkowsi and Lambourne (64-65) used a surface balance technique to measure the steric repulsive forces arising from polymer layers adsorbed on polymethyl methacrylate particles in different dispersion media. Andrew et al. (66) used a capacitance technique to measure the change in film thickness as a function of applied potential and calculated the steric repulsive forces. Homola and

Robertson (67) used compression by hydrostatic pressure of a colloidal dispersion confined between a semipermeable membrane and an immiscible liquid to measure the electrostatic and steric repulsive forces; the equilibrium pressures and volumes were measured, and the potential energy curves were calculated. Ottewill et al. (68) recently extended the disjoining pressure technique to measure the repulsive pressure resulting from the interaction of two surfaces with adsorbed polymer layers.

1.2.5 Electrostatic, Steric, and Electrosteric Stabilization

The treatment of electrostatic stabilization is based on the DLVO theory developed by Derjaguin and Landau (40-43), and Verwey and Overbeek (39). According to this theory, the scalar repulsive and attractive forces are simply added to give the total interaction energy. The repulsive and attractive forces are distance-dependent functions. For the range of the individual components for particles of infinite size, the dispersion energy decreases proportionally to 1/d, while the electrostatic energy decreases exponentially. Thus the attractive energy is predominant at very small and great distances, and the electrostatic energy is predominant at intermediate distances, to give a potential energy-distance diagram of the type shown in Figure 1.2. At very small distances, there is a primary minimum of coagulation (attractive forces predominant); at intermediate distances, a stability peak (repulsive forces predominant); at greater distances

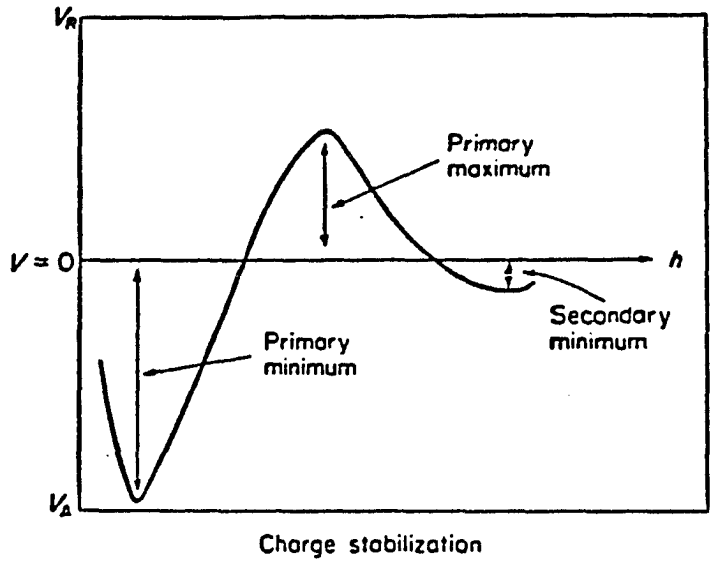

Figure 1.2 Potential energy (V) curve as a function of distance of separation (h) for electrostatic stabilization (ref: 68a).

beyond the range of electrostatic stabilization, a secondary minimum of flocculation (attractive forces predominant).

The treatment of steric stabilization is based on the HVO theory of Hesselink, Vrij and Overbeek (39) in which the attractive and steric repulsive forces are added to give the total interaction energy. According to this theory, the steric repulsive energy is a combination of two energies, one arising from the volume restriction effect and the other from the mixing effect. For the combined electrosteric stabilization, no theory has been developed to date to give the total interaction energy. Instead, the scheme of the DLVO theory is usually followed by simply adding the various interaction energies to give the total interaction energy. Figure 1.3 shows the potential energy diagram resulting from the superposition of the steric repulsive energy on the attractive energy. One distinct feature of this diamgram is the absence of a primary minimum, which is due to the fact that, as the particles approach one another, the ever-increasing steric repulsive energy masks the attractive energy.

Unlike electrostatic repulsion, steric repulsion falls to zero at a finite distance. Certain combinations of polymer layer thickness and particle size give a secondary minimum of flocculation. For electrosteric repulsion, various types of potential energy-distance plots can be constructed according to the relative contributions of these components. Figure 1.4 shows one such plot in which the electrostatic

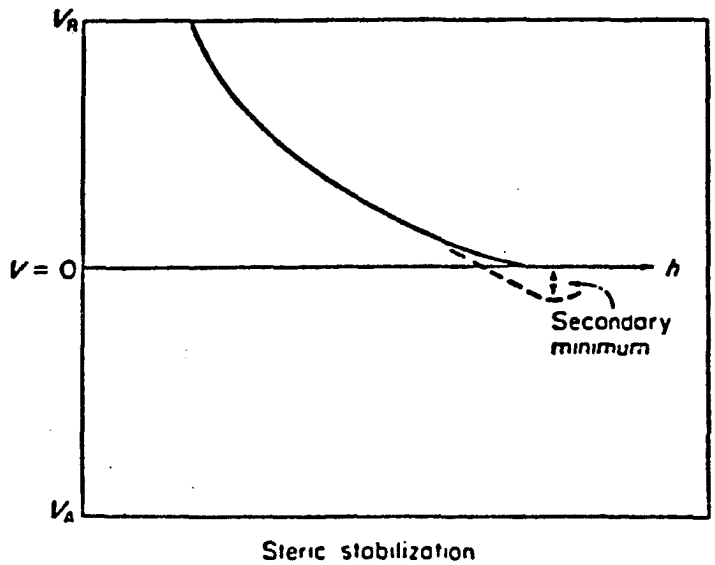

Figure 1.3 Potential energy (V) curve as a function of distance of separation (h) for steric stabilization (ref: 68a).

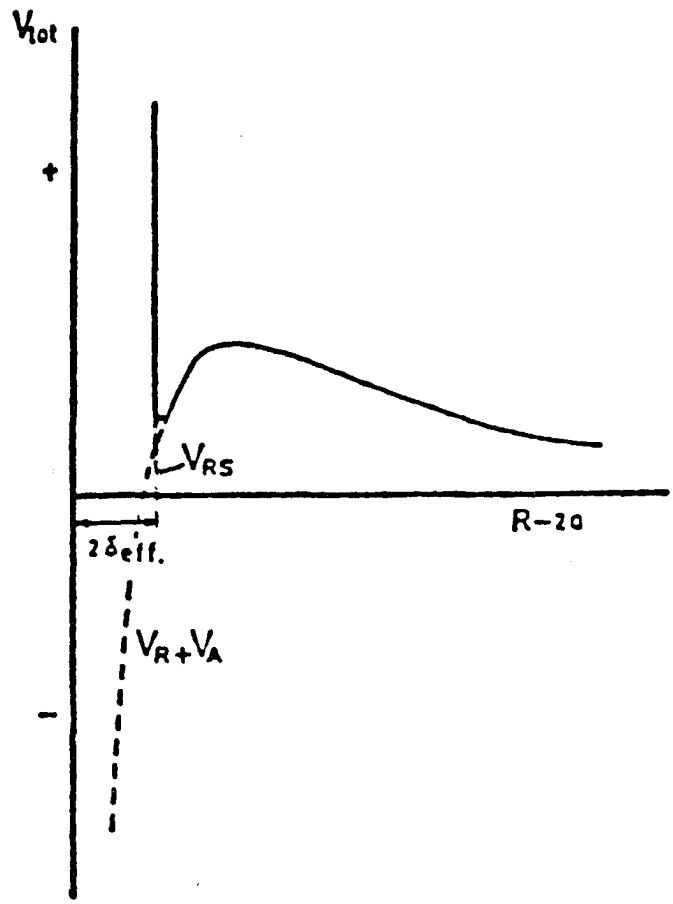

Figure 1.4 Potential energy (V) curve as a function of distance of separation (h) for the electrostatic stabilization (ref: 68a).

repulsion is operative over a long range, so that as long as the repulsive barrier is high enough to prevent close approach of the particles, the effect of the steric repulsion would not be seen; however, the particles surmounting the electrostatic repulsion barrier would fall into a primary minimum at a distance of less than twice the adsorbed layer thickness; in this case, the flocculated particles could be repeptized, provided that the primary minimum is not too deep relative to stability peak.

1.3 Scope and Objectives of the Present Work

The objectives of this study were as follows.

(i) To demonstrate the applicability of the serum replacement technique to measure polymer adsorption.

(ii) To investigate the adsorption of a typical water-soluble surface-active polymer on polystyrene latex particles.

(iii) To determine the effect of the adsorbed polymer on the colloidal stability.

Polyvinyl alcohol was chosen as the adsorbate because of its wide use in industry, and monodisperse polystyrene latex particles as the adsorbent because of their well-characterized surfaces. The solution properties of polyvinyl alcohol were investigated to determine the state of the polymer coil, not only because of its known effect on adsorption, but also because of the conflicting reports in the literature. Wherever possible, all parameters were measured by at least two

techniques. The solution properties were measured by differential refractometry, viscometry, electron microscopy, and gel permeation chromatography. The adsorption isotherms were measured by the adsorption and desorption methods of the serum replacement technique. The adsorbed polymer layer thickness was measured by viscometry and photon correlation spectroscopy. The heats of adsorption were measured by microcalorimetry.

The variation of three parameters was investigated: (i) the molecular weight of the polyvinyl alcohol; (ii) its degree of hydrolysis; (iii) the particle size of the polystyrene substrate. High polyvinyl alcohol concentrations and long equilibration times were used to attain adsorption equilibrium, which gave some features which were not recognized in the past. No systematic investigation of the effect of substrate particle size on the adsorption has been reported in the literature, perhaps because of the difficulties in cleaning and handling the larger-particle-size latexes. As a good representation of the colloidal range, monodisperse polystyrene latexes of three particle sizes - 190nm, 400nm, and 1100nm - were used. The cleaning problem was overcome by diluting the latexes to very low solids for cleaning, followed by concentration after cleaning.

To study the effect of the adsorbed polymer on the colloidal stability, monodisperse polystyrene latexes of two particle sizes - 190nm and 400nm - were used. Electrolyte

stability measurements were made for the bare and the polyvinyl alcohol-covered particles. Similar measurements were carried out in the past for particles stabilized with low-molecular-weight emulsifiers where the possibility of desorption during the experiments cannot be ruled out. With the polyvinyl alcohol-covered particles, these measurements may be more meaningful because of the absence of desorption on dilution. There are few direct experimental methods to measure the repulsive forces between colloidal particles. A simple adaptation of the serum replacement cell was used to measure the repulsive forces between the bare and the polyvinyl alcohol-covered particles.

2. EXPERIMENTAL

2.1 Materials

1. General. All chemicals used were certified analytical grade reagents. The water used was doubly-distilled and deionized (DDI) and had a conductivity of 0.4μm mhos per centimeter. Pyrex glassware was used throughout.

2. Dowex 50W and Dowex 1 Ion Exchange Resins. The latexes were cleaned using the Dowex 50W (H^+ form of sulfonated 96:4 styrene-divinylbenzene copolymer; Dow Chemical)-Dowex 1 (OH^- form of analogous trimethylammonium derivative) mixed resin. Each resin was cleaned (69,70) by washing consecutively with 3N sodium hydroxide, hot water, methanol, cold water, 3N hydrochloric acid, hot water, methanol, and cold water. This cycle was repeated four times until the conductivity, absorbance at 224nm, and surface tension of the wash water reached the desired (69) values.

3. Polystyrene Latexes (PS). The latexes used were the Dow monodisperse polystyrene latexes LS-1102-A, LS-1103-A, and LS-1166-B with average particle diameters of 190, 400, and 1100nm, respectively. The latexes were cleaned by ion exchange with mixed Dowex 50W-Dowex 1 resins (71). The surface groups of the ion-exchanged latexes determined by conductometric titration (70) were strong-acid sulfates; the surface charge densities were 1.35, 3.00, and 5.95 μC/cm^2, respectively.

4. Polyvinyl Alcohols (PVA). The polyvinyl alcohols used were commercial Vinol samples (Air Products & Chemicals). Table 2.1 gives the specifications of these samples.

TABLE 2.1

SPECIFICATION OF POLYVINYL ALCOHOL (VINOL) SAMPLES

GRADE	HYDROLYSIS %	VISCOSITY CPS*	$\bar{M}n$	$\bar{M}w$
Vinol 107	98.0-98.8	5-7 (Low)	23,000	35,800
Vinol 325	98.0-98.8	28-32 (Medium)	80,000	118,100
Vinol 350	98.0-98.8	55-65 (High)	107,150	161,600
Vinol 205	87.0-89.0	4-6 (Low)	26,400	34,500
Vinol 523	87.0-89.0	21-25 (Medium)	79,100	120,400
Vinol 540	87.0-89.0	40-50 (High)	110,000	164,500

*4% Aqueous Solutions at 20°C.

The polyvinyl alcohol solutions were prepared by dispersing the powdered polymer in water at room temperature using sufficient agitation to wet all of the particles. After the particles were well dispersed, the temperature was raised to 95°C for the fully hydrolyzed grades and to 80°C for the partially hydrolyzed grades. The heating was continued until all of the polyvinyl alcohol was dissolved. The clear solutions were filtered hot through Whatman filter paper and cooled. The polyvinyl alcohol contents were determined gravimetrically. Freshly prepared solutions were used for all experiments. All solutions were discarded 36 hours after preparation.

2.2 Techniques

2.2.1 Solution Properties of Polyvinyl Alcohol

Four independent techniques were used to determine the solution properties of polyvinyl alcohol: a) differential refractometry; b) viscometry; c) transmission electron microscopy; d) gel permeation chromatography.

a) Differential Refractometry. The Brice-Phoenix Model BP-2000-V Differential Refractometer was used to measure the difference in refractive index between a dilute solution of polyvinyl alcohol and water. The instrument consists of four components: a light source; cell housing; mirrors and lenses; and a microscope. All four components were mounted on a rigid cast-aluminum optical bench. The light source was a type AH-3 mercury vapor lamp operated by a 115-volt 60-cycle line transformer. The lamp housing was equipped with a filter turret with two filters for isolating either the blue (436nm) or green (546nm) wavelengths.

The monochromatic light beam passes through the semi-transparent mirror and a vertical slit of adjustable width into the entrance window of the jacketed cell housing. The sinterfused optical glass cell comprised a 15-mm square cross-section with plane parallel windows, a removable cover, and a 1.2-mm thick diagonal glass partition which divides the cell into two equal-volume compartments, one for the solvent and the other for the polymer solution. The cell holder inside the housing could be rotated 180° about

the vertical axis by means of a handle projecting from the fixed housing. The light beam passing through the cell and out the exit window is bent through an angle proportional to the refractive index difference between the two liquid samples. The image of the slit is projected onto the focal plane of the objective of a microscope equipped with a micrometer eyepiece with a 10-mm fixed scale and a drum divided in 0.01-mm units. The microscope can be moved along its longitudinal axis, allowing focal adjustment of the slit image. This instrument is ideal for the measurement of refractive indices up to values of 1.62 and for refractive index differences up to about 0.01 units. The refractive index of a dilute polymer solution varies only gradually with concentration so that the differential refractive index-concentration plots should be linear.

b) Viscometry. The viscosities of the polyvinyl alcohol solutions were measured using a Cannon-Ubbelohde capillary viscometer (capillary constant 0.01). The temperature variation during the measurements was less than 0.05°C. The efflux time was measured by visual observation of the drainage of the liquid meniscus past the two lines marked on the viscometer capillary timed with a stopwatch. The efflux time for pure water was 98 sec. The kinetic and shear corrections were negligible. The intrinsic viscosities $[\eta]$ and the Huggins constants K' of the polyvinyl alcohol samples were determined from Huggins

equation:

$$\eta_{sp}/c = [\eta] + K' [\eta]^2 c \qquad 2.1$$

where η_{sp}/c is the reduced specific viscosity and c the polymer concentration in the solution. The viscosity-average molecular weights $\langle M_v \rangle$ were calculated from the intrinsic viscosities using the Mark-Houwink-Sakurada (MHS) relationship:

$$[\eta] = K \bar{M}_v^{a} \qquad 2.2$$

where K and a are constants which depend upon the polymer, solvent, and temperature. The unperturbed dimensions of the polymer chains can be calculated from random-flight statistics. The simplest model which places no restriction on bond rotation or bond angles gives for the root-mean-square (r.m.s.) end-to-end distance:

$$(\bar{r}_o^2)^{\frac{1}{2}} = \ell n^{\frac{1}{2}} \qquad 2.3$$

where ℓ is the carbon-carbon bond length (1.54Å.) and n the number of links (~2dp). If the restriction of constant bond angle is imposed, the expression becomes:

$$\bar{r}_o^2 = n\ell^2 \frac{(1-\cos\theta)}{(1+\cos\theta)} \sim 2n\ell^2 \qquad 2.4$$

where θ is the bond angle (109° for tetrahedral geometry). The imposition of a further restriction of a barrier to free bond rotation (which represents the actual case under θ conditions) gives:

$$\bar{r}_o^2 = n\ell^2 \frac{(1-\cos\theta)}{(1+\cos\theta)} \sigma^2 \qquad 2.5$$

where σ is called the steric factor. The molecular dimensions of the polymer coils in solution can be determined from the intrinsic viscosity using the Burchard-Stockmayer-Fixman (BSF) (72-73) relationship:

$$[\eta]M^{-\frac{1}{2}} = K_\theta + 0.51\ \Phi_o\ B\ M^{\frac{1}{2}} \qquad 2.6$$

where

$$K_\theta = \Phi_o\ [(r_o^2)/M]^{3/2} \qquad 2.7$$

$$B = \beta\ M_s^{-2} = v^2\ (1-2\chi)\,(V_1 N_A)^{-1} \qquad 2.8$$

where Φ_o is the universal constant having a value of 2.8×10^{21} dl (gm mole^{-1}) cm^{-3}, M the molecular weight of the polymer, $\bar{r}_o^2$ the unperturbed root-mean-square end-to-end distance, B the binary cluster integral for a pair of segments, M_s the molecular weight of a segment, v the specific volume of the polymer, χ the Flory interaction parameter, V_1 the molar volume of the solvent, and N_A Avogadro's number. If the intrinsic viscosities of a series of polymers of different molecular weights are know, K_θ can be calculated from the intercept of the $[\eta]M^{-\frac{1}{2}}$ - $M^{\frac{1}{2}}$ plot of equation 2.6. The unperturbed dimensions of the coil can then be calculated from Equation 2.7. In the derivation of the BSF relationship, the heterodispersity of the polymer molecular weights is not considered. Koopal (74) has taken this heterodispersity into account and has derived a corrected equation; however, for samples with similar molecular weight distributions, the heterodispersity correction becomes constant

and Equation 2.6 can be used. The perturbed molecular dimensions of the polymer coil can also be determined from the same intrinsic viscosity data using the relationship:

$$[\eta] = \Phi \frac{(\bar{r}^2)^{3/2}}{M} \qquad 2.9$$

where $\Phi \lesssim \Phi_o$ is the universal constant and M the molecular weight of the polymer.

c) Transmission Electron Microscopy (TEM). The polyvinyl alcohol solutions were investigated using the cold-stage freezing technique. A hemispherical drop of the diluted polymer solution was placed on an electron microscope specimen substrate, and most of the drop was removed using filter paper to leave a thin film; the sample was then frozen at liquid nitrogen temperature and placed in a special sample holders which maintained the sample at liquid nitrogen temperature inside the electron microscope; the sample was then evacuated and examined while still frozen. Freezing the sample at liquid nitrogen temperature allows examination of the structural features of the dilute polyvinyl alcohol solutions.

d) Gel Permeation Chromatography (GPC). GPC measurements were carried out at 25°C using a Waters Associates Model 201 A 6PC Gel Permeation Chromatograph. This instrument comprises a solvent reservoir, pump, packed columns, differential refractometer detector, and associated equipment. The solvent stream is divided and pumped through a

dummy column to provide the pressure drop, the reference side of the detector, and the separation columns to the sample side of the detector. The samples are injected into the solvent stream with an injection loop and a valve. The concentration of the polymer solutions was about 0.25 gm/100 cm^3 and the flow rate was 1 cm^3/sec. The 300mm-long 7.5mm-internal diameter TSK-GEL (Toyo Soda Manufacturing Co., Ltd.; type-PW of G6000PW, G5000PW, and G3000PW) columns were packed with 15μm-diameter semi-rigid particles of a hydrophilic polymer gel. This instrument gave high-speed aqueous gel permeation chromatographic separations of good resolution without adsorption of the polyvinyl alcohol on the column packing. The instrument was calibrated using dextran and polyacryl amide standards of known molecular weights. (10^3-10^6).

2.2.2 Adsorption Isotherms

The serum replacement technique (75) was used to determine the adsorption isotherms of the polyvinyl alcohols on the polystyrene latex particles. The latex was confined in a cell with a semipermeable membrane which allowed passage of polyvinyl alcohol molecules but not the latex particles; pure water was pumped through the cell to remove the unadsorbed and desorbing polyvinyl alcohol, leaving the latex particles in the cell. These measurements used a commercial cell (Nuclepore Corp.) comprising an inlet and an outlet, a magnetic stirrer, and a porous disc to support

the semipermeable membrane. The semipermeable membranes used were the uniform pore-size Nuclepore filtration membranes; the pore size of the membrane was usually about 75% of the particle diameter of the monodisperse polystyrene latex. The adsorption isotherm can be determined by two methods: adsorption or desorption. In the adsorption method, polyvinyl alcohol adsorbate solutions of different concentration are added to latex samples of the same concentration and allowed to equilibrate; the samples are then placed in the serum replacement cell, and a small volume of aqueous serum is removed and analyzed, to construct the adsorption isotherm. In the desorption method, a latex sample containing a known concentration of polyvinyl alcohol adsorbate is confined in the cell, and pure water is pumped through the cell to remove the unadsorbed and desorbed adsorbate. The flow of the feed and exit streams is maintained at a slow constant rate to ensure equilibrium. The exit stream is monitored using a suitable detector (differential refractive index monitor for polyvinyl alcohol) to determine the concentration of desorbing adsorbate. A mass balance on the added amount of adsorbate is then carried out to construct the adsorption isotherm. Figure 2.1 shows a schematic diagram of the desorption experiment. The advantage of the desorption method over the adsorption method is that the adsorption isotherm is generated in a shorter time using a single sample.

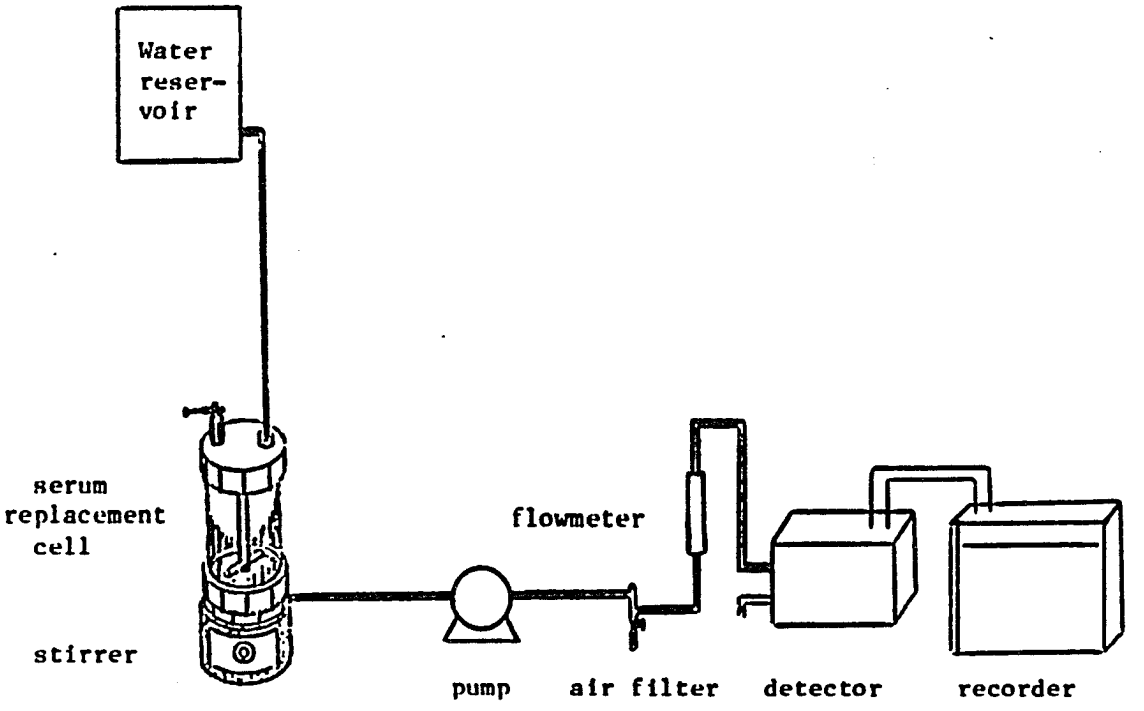

Figure 2.1 Schematic diagram of the apparatus used for desorption experiments.

2.2.3 Thickness of the Adsorbed Layer

Two techniques were used to measure the thickness of the adsorbed polyvinyl alcohol layer on the polystyrene latex particles: a) viscometry; b) photon correlation spectroscopy.

a) Viscometry. This method is based on the principle that the viscosity of a dispersion depends on the volume fraction of the dispersed particles. If the volume fraction of the dispersed spherical particles is small, the variation of viscosity with volume fraction is linear as given by the Einstein equation:

$$\eta_{red}/\phi = K_E + k'K_E^2\phi \qquad 2.10$$

where η_{red}/ϕ is the viscosity ratio excess, ϕ the volume fraction of spheres, k' the Huggins constant, and K_E the Einstein coefficient, which depends on the shape of the particles and is 2.5 for solid uncharged spheres. The presence of an adsorbed polymer layer on the particles increases the effective volume fraction (ϕ^*) by a factor f:

$$\phi^* = f\phi \qquad 2.11$$

The Einstein equation for spheres covered with an adsorbed polymer layer would then become:

$$\eta_{red}^*/\phi = K_E f + k'(K_E f)^2\phi \qquad 2.12$$

A plot of the left-hand side of Equation 2.12 against ϕ should give a straight line with a slope k' $(K_E f)^2$ and an

intercept $K_E f$. Assuming that the adsorption of a polymer layer does not change the shape of the sphere, f can be calculated from the difference in the intercepts of the viscosity plots for the bare and the covered spheres; f can then be related to the thickness of the adsorbed layer from the relationship:

$$\delta = R\ (f^{1/3}-1) \qquad 2.13$$

where δ is the adsorbed layer thickness and R the radius of the bare particle. The Cannon-Ubbelohde capillary viscometer (capillary constant 0.01) was used to measure the viscosity of the polystyrene latexes at 25.00±0.05°C. The latex samples were cleaned using serum replacement, and part of the latex serum was separated; the relative viscosity of the serum was virtually the same as that of the DDI water, so that either could be used for diluting the latex samples for the viscosity measurements. The viscosity of the cleaned latexes was measured to give a standard for the bare particles, i.e., without an adsorbed layer of polyvinyl alcohol. For the samples with an adsorbed layer of polyvinyl alcohol, samples from the plateau region of the adsorption isotherm were washed further with water until no polyvinyl alcohol was detected in the serum by differential refractometry. The relative viscosity of the serum of these samples was also virtually the same as that of the DDI water. The most concentrated samples (ϕ = 0.025) were diluted with DDI water and their viscosities were mea-

sured. Dilution of these samples did not result in desorption of the polyvinyl alcohol because of the irreversible nature of its adsorption. 1mM aqueous sodium chloride was added to the negatively charged polystyrene latexes to suppress the electroviscous effect. The electrolyte concentration was not adjusted to constant ionic strength during dilution because of the possibility of flocculation of the particles, which was observed by Fleer (76).

b) Photon Correlation Spectroscopy. This technique is based on the fact that the intensity of the scattered light fluctuates continuously around its mean value owing to the Brownian motion of the particles. In these experiments, the autocorrelation function $C(\tau)$ of these time-dependent intensity fluctuations of the scattered light is determined. For a monodisperse latex, the autocorrelation function $C(\tau)$ decays as a single exponential with a characteristic correlation time τ_c(77). In a homodyne light scattering experiment (78), the correlation time τ_c can be related to the translational diffusion coefficient D_T of the particles by:

$$\tau_c = (2K^2 D_T)^{-1} \qquad 2.14$$

where the parameter K is given by:

$$K = \frac{4\pi n_s \, \mathrm{Sin}(\theta/2)}{\lambda} \qquad 2.15$$

where n_s is the refractive index of the scattering medium, θ the scattering angle, and λ the wavelength of the light source. The Stokes-Einstein relationship for monodisperse

spheres can be used to determine the hydrodynamic diameter from the translational diffusion coefficient:

$$D_T = \frac{kT}{3\pi\eta d} \qquad 2.16$$

where k is the Boltzmann constant, T the absolute temperature, and η the viscosity of the scattering medium.

The photon correlation spectroscopy measurements were made using the Chromatix KMX-6DC low-angle light-scattering photometer. The photometer was attached to a 64-channel digital correlator and interfaced with a PDP-1103 data processing system (Digital Equipment). The light source was a 2mW He-Ne laser (λ_o = 632.8nm). The instrument gives accurate measurements within 1-2 minutes after proper alignment. The instrument was aligned using the procedure of Derderian et al (79). The concentration of the latex samples was 0.005-0.020%. The sodium chloride concentration used was 1mM (the same as that used in the viscosity measurements). All measurements were made at ambient temperature at an angle of 174°.

2.2.4 Heats of Adsorption

The heats of adsorption of polyvinyl alcohol on the polystyrene latex particles were measured using the Tronac Model 1250-Isothermal Microcalorimeter. This automated microcalorimeter comprises four components: an electronic console for temperature sensing; a thermostated water bath with an insert assembly; analog and digital outputs; a

computer interfaced with a teleprinter to control the sample injection and data handling. The insert assembly holds the reaction vessel with a stirrer and the titrant burette. The temperature of the bath is controlled to within ±0.003°C. The insert assembly is placed in the water bath so that the titrant and the reaction vessel are maintained at constant temperature. The reaction vessel comprises a stainless-steel or platinum inner cup inside a water-tight stainless-steel container. Under the cup and inside the container are a water control heater and a Peltier thermoelectric cooler. Heat is removed from the reaction vessel to the outer bath at a constant rate (adjustable) through the Peltier cooler. Heat enters the reaction vessel in the form of fixed energy pulses from the control heater to keep the internal temperature constant. The water bath in which this vessel is immersed also has a similar arrangement. During a run, the Peltier cooling rate is maintained constant. Since the instrument is operated under isothermal conditions, fewer heat pulses are needed to keep the temperature of an exothermic reaction constant; conversely, more pulses are needed to keep the temperature of an endothermic reaction constant. The heat evolved is calculated from the difference in the requisite number of heater pulses using the appropriate electrical calibration data.

The calorimeter was calibrated using the chemical reaction between tris(hydroxymethyl)aminomethane (THAM) and

hydrochloric acid. This reaction has been well studied and is recommended as a calibration reaction for the microcalorimeter. For the heats of adsorption of polyvinyl alcohol on polystyrene latex particles, the polyvinyl alcohol concentrations were sufficient to give saturation adsorption. The 190nm-diameter polystyrene latex was used in dilute concentration (0.25%); for the latexes of larger particle size, the particle concentration was adjusted so as to have the same total surface area. Experimental runs were made over periods of time. For a normal run, the polyvinyl alcohol solution was added continuously at a rate of 0.0985 cm^3/ minute over a period of 15 minutes, and the heat evolved was measured. For other runs, the polyvinyl alcohol solution was added initially, and the heat evolved was measured over a period of 15 hours. The heats of dilution of the polyvinyl alcohol solutions were negligible over these time periods.

2.2.5 Electrolyte Stability

The electrolyte stability of the bare and PVA-covered latexes was measured from the rate of flocculation upon addition of aqueous sodium chloride solution. The measurements were carried out using a Beckman 5270 spectrophotometer equipped with a 1-cm pathlength 4-cm^3 capacity cell and an optical density-time recorder set at 1370nm, the longest wavelength. The use of light wavelengths in the infrared region allows the interpretation of data using the

simple Rayleigh theory of light scattering. Aqueous sodium chloride solutions were injected into the sample cell using a 1-cm^3 syringe. The quick injection was considered sufficient to thoroughly mix the electrolyte solution with the latex. The latex particle concentration in the sample cell was 0.015%. The latex particle concentration in the reference cell was such that the concentrations in both cells were the same after the addition of electrolyte solution. The principle of this method is that the initial slope (time = 0) of the optical density-time curve is proportional to the rate of coagulation. This initial slope increases with increasing electrolyte concentration until it reaches a limiting value. The stability ratio W is defined as the ratio of the limiting initial slope to the initial slope measured at lower electrolyte concentrations. The log W-log electrolyte concentration plot shows a sharp inflection point at the critical coagulation concentration (W = 1), which is a measure of the stability of the latex to added electrolyte. Reerink and Overbeek (80) have shown that the value of W is determined mainly by the height of the primary repulsion maximum in the potential energy-distance curve.

2.2.6 Electrophoretic Mobility

The electrophoretic mobilities of the bare and PVA-covered latex particles were measured using the automated Pen Kem 3000 system. The particles are placed in a cylin-

drical capillary cell and illuminated by a laser light beam positioned perpendicularly to the cell and focused at the stationary flow level. The light scattered by the particles at 90° to the incident beam is collected and focused on a rotating grated disk. The pulses of light passing through the disk impinge upon a photomultiplier tube, the output of which is analyzed by a spectrum analyzer to give a frequency difference spectrum. The system takes multiple averages of the population of particles undergoing electrophoresis and gives a distribution of frequencies, which is proportional to the electrophoretic mobility distribution of the sample.

2.2.7 Repulsive Forces

A serum replacement cell was used to measure the repulsive forces between the latex particles. This method is based on the fact that the stepwise application of pressure to a latex sample confined in a cell with a semipermeable membrane decreases the interparticle distance so that the latex particles are forced into packed arrays, with the interparticle repulsive forces balancing the applied pressure. If the applied pressure is high enough to overcome the repulsive forces, the latex particles coagulate to give a maximum in the pressure-volume curve. For spherical particles, the interparticle repulsive forces can be estimated from the maximum in the pressure-volume curve. This method is similar in principle to that used by Ottewill

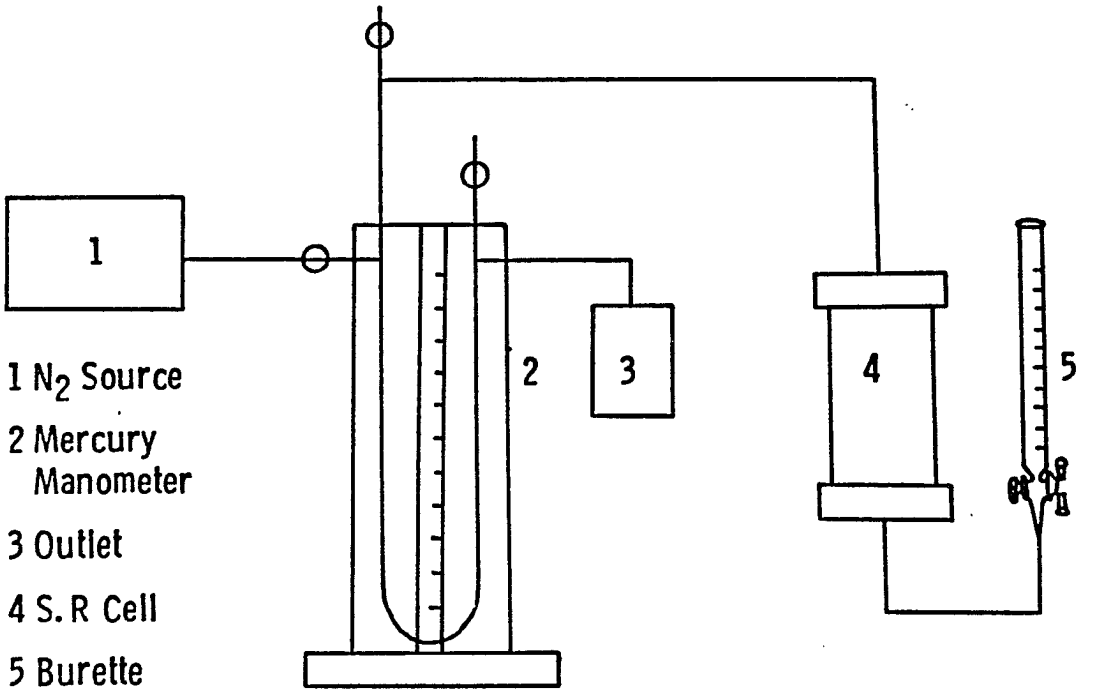

Figure 2.2 Schematic diagram of the apparatus used for repulsive force measurements.

et al. (61,68) but uses a much simpler experimental apparatus (Figure 2.2), comprising a nitrogen gas source to exert the pressure, a mercury manometer to measure the pressure, a serum replacement cell, and a burette to measure the change in volume. Latex samples of 18-20% solids (the maximum concentration achieved by gravitational separation of the serum using the cell) containing 5 gm particles were placed in the cell. A constant pressure was applied stepwise, and the change in volume of the serum in the burette was measured, to give the variation of particle volume fraction with pressure.

3. SOLUTION PROPERTIES OF POLYVINYL ALCOHOL

3.1 Introduction

Polyvinyl alcohol (PVA) is a peculiar polymer in that it has a simple chemical structure but varying properties, even with samples of the same specifications. Nevertheless, it has achieved widespread use in the United States, e.g., in textile sizing (40%), adhesives (25%), paper coating (13%), and emulsifiers (10%), according to a recent survey (81). Polyvinyl alcohol cannot be prepared by polymerization of its monomer; it is prepared by hydrolysis of polyvinyl acetate. Polyvinyl alcohols of different degrees of hydrolysis are available. The requisite degree of hydrolysis depends upon the particular application, e.g., high degrees of hydrolysis (ca. 100%) are required for its application in adhesives, textiles, and paper coating, whereas a degree of hydrolysis of 88% is preferred for its use as a surface-active agent. Polyvinyl alcohol is a crystalline polymer; however, once it is dissolved in a solvent, its crystallinity is destroyed. The conformation of the polymer chain in solution, i.e., the size and the symmetry of the polymer coil, is determined by the nature of the solvent. One conflicting view of aqueous polyvinyl alcohol solutions is that the polymer forms globules at low concentrations and networks of chainlike aggregates of these globules at higher concentrations (82). The formation of

these networks in aqueous polyvinyl alcohol solutions would have a profound effect on the adsorption of polyvinyl alcohol on colloidal particles. Therefore, it was essential to investigate the state of dispersion of the polyvinyl alcohol molecules in dilute aqueous solution. Four independent techniques were used: a) differential refractometry; b) viscometry; c) transmission electron microscopy; d) gel permeation chromatography. Since the adsorption experiments were carried out using dilute solutions, the concentrations used for these investigations were low-to-moderate (0.05-4.0%).

3.2 Results and Discussion

3.2.1 Differential Refractometry

Figure 3.1 shows the variation of refractive index $\Delta\eta$ with concentration up to 0.26% for the fully hydrolyzed polyvinyl alcohols. It can be seen that the $\Delta\eta$-C plots were linear and the data for the various polyvinyl alcohol samples fell on the same line. Matsumoto et al. (83) studied the concentration dependence of the refractive index of fully (98-100%) hydrolyzed polyvinyl alcohols; their $\Delta\eta$-C plots (Figure 3.2) showed an abnormal change in slope at certain polyvinyl alcohol concentrations, which they attributed to a change in the state of dispersion of the polyvinyl alcohol molecules. This abnormal change in refractive index shifted to lower concentrations with increasing polyvinyl alcohol molecular weight over the range 1.95-

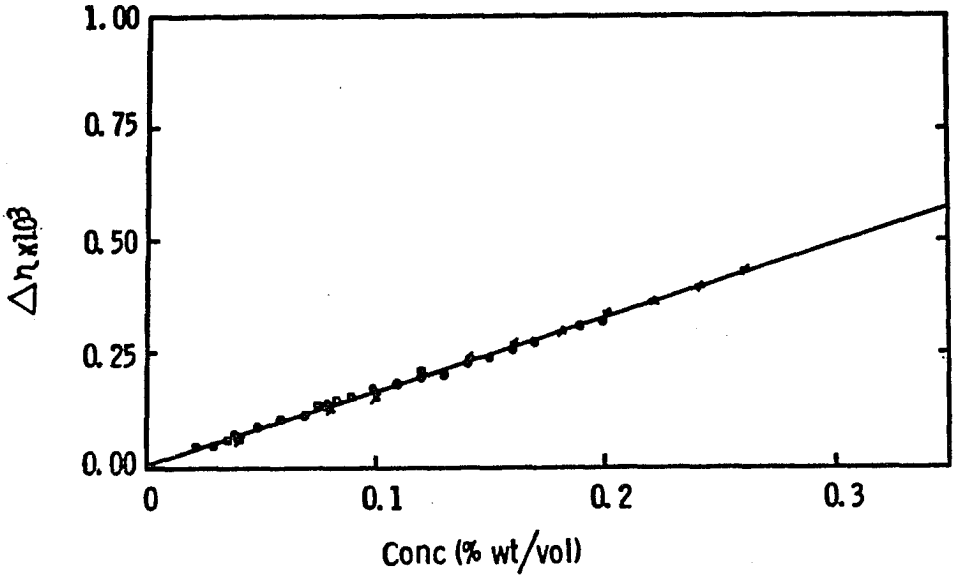

Figure 3.1 Δη versus concentration for aqueous solutions of polyvinyl alcohol at 25°C: (o-o) Vinol 107; (x-x) Vinol 325; (□-□) Vinol 350.

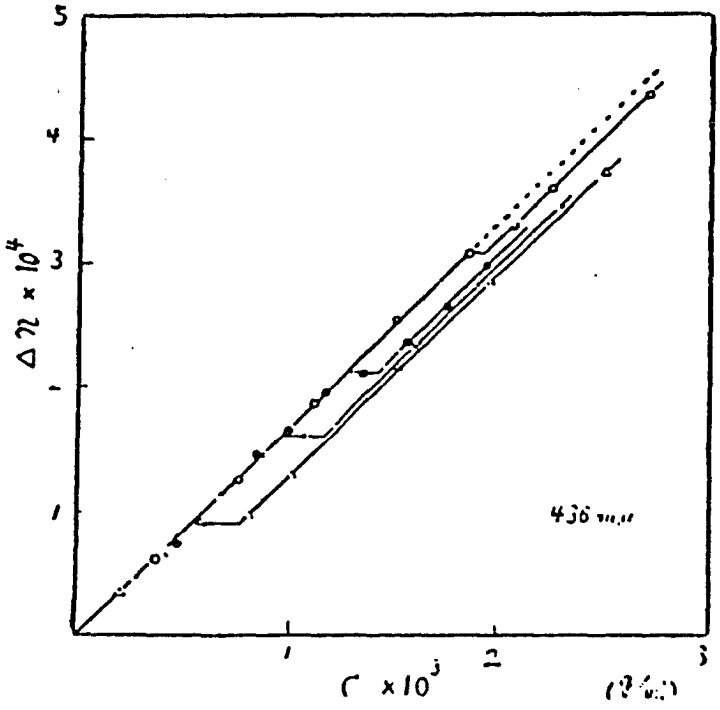

Figure 3.2 Δη versus concentration for aqueous solutions of polyvinyl alcohol (fully hydrolyzed) at 30°C: dp = 145 (o); 880 (●); 1182 (x); and 4210 (Δ); ref: 83.

18.5×10^4. In the present study, however, no such abnormal change in slope was observed; therefore, the possibility of structure formation was ruled out.

3.2.2 Viscometry

Figure 3.3 shows that the variation of reduced specific viscosity with concentration was linear over a wide concentration range. According to the Huggins relationship, the extrapolation of these lines to zero concentration gives the intrinsic viscosity $[\eta]$. The Mark-Houwink-Sakurada (MHS) equation can be used to calculate the viscosity-average molecular weight from the intrinsic viscosity if the values of the constants K and a are known. Various values of K and a have been reported (75,84-88) for polyvinyl alcohol solutions. The values of these constants depend upon the nature of the polymer and the solvent, and the temperature. The constant a is a measure of the polymer-solvent interaction and varies from 0.5 for θ solvents to 0.8-1.0 for linear polymers in good solvents (89-91). The constant K depends upon the nature of the polymer. The values of these constants depend upon the degree of hydrolysis of the polyvinyl alcohol. Beresniewics (85) found that a decreased strongly and K increased with decreasing degree of a hydrolysis, whereas Garvey et al. (88) found a higher value of a and lower value of K for the partially hydrolyzed polyvinyl alcohols as compared with fully hydrolyzed samples. In this study, single values of a and K were sufficient to characterize the molecular weights of both

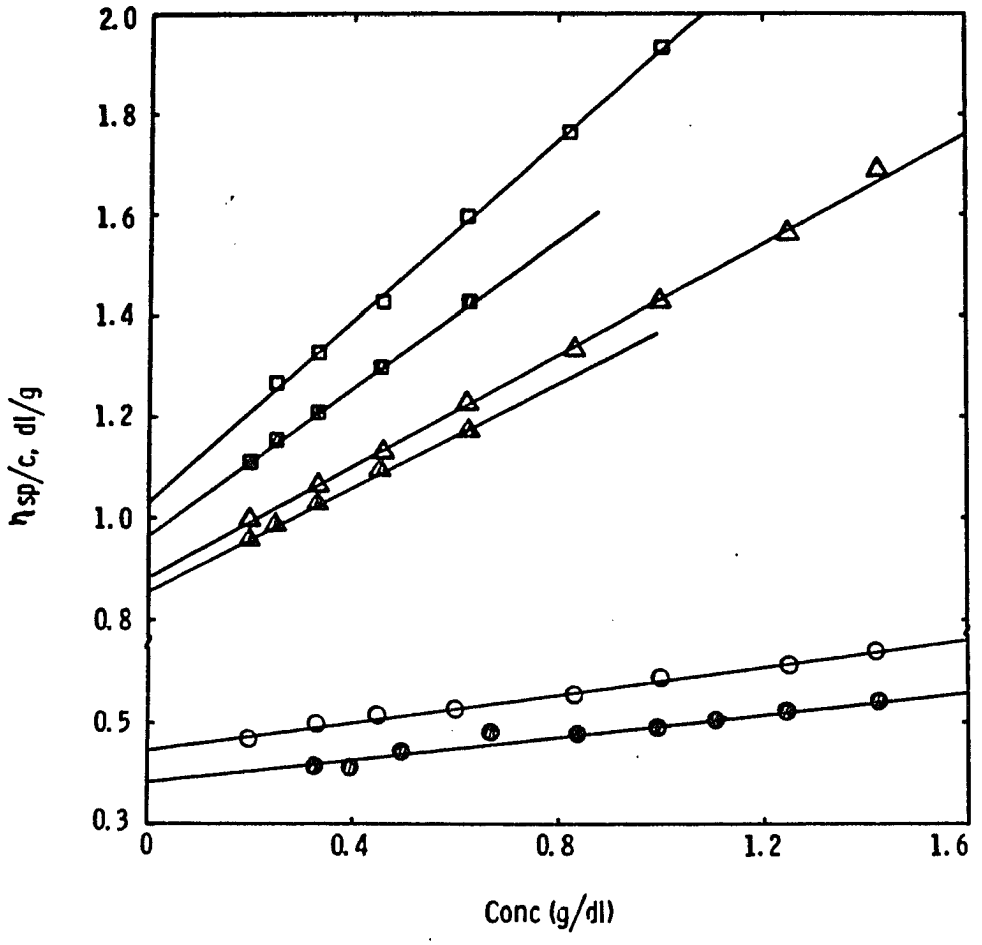

Figure 3.3 Reduced viscosity versus concentration for aqueous solutions of polyvinyl alcohol at 25°C: (o) Vinol 107; (ø) Vinol 205; (Δ) Vinol 325; (Å) Vinol 523; (□) Vinol 350; (▣) Vinol 540.

the fully hydrolyzed and partially hydrolyzed polyvinyl alcohols. With these constants, the MHS equation becomes:

$$[\eta] = 5.95 \times 10^{-4} \bar{M}v^{0.63} \qquad 3.1$$

Table 3.1 gives the intrinsic viscosities, the Huggins constants k', and the viscosity-average molecular weights determined using the MHS equation as well as the weight-average molecular weights determined by gel permeation chromatography for the various polyvinyl alcohols. The viscosity-average molecular weights were lower or close to the weight-average molecular weights as expected. The value of k' varied from 0.60 to 0.85 for the fully hydrolyzed polyvinyl alcohols, and from 0.66 to 0.78 for the partially hydrolyzed polyvinyl alcohols. No attempt was made to interpret the values of k' because these values have no theoretical significance.

TABLE 3.1

INTRINSIC VISCOSITY, k' & MOLECULAR WEIGHTS AT 25°C

SAMPLE	[η]dℓ/g	k'	$\bar{M}_v$	$\bar{M}_w$
Vinol 107	0.4470	0.60	36,700	35,800
Vinol 325	0.8807	0.70	107,700	118,100
Vinol 350	1.0293	0.85	138,000	161,600
Vinol 205	0.3871	0.66	29,200	34,500
Vinol 523	0.8669	0.65	105,000	120,400
Vinol 540	0.9666	0.78	124,850	164,500

Table 3.2 shows the unperturbed molecular dimensions under various structural constraints. The dimensions for the freely rotating and constant bond-angle conditions were calculated using Equations 2.3 and 2.4. These equations do not take into account any steric hindrance to free rotation of the polymer coil. The experimental values calculated from the intrinsic viscosities, however, show these effects. Under non-theta conditions, the polymer chains have perturbed dimensions; however, the unperturbed dimensions can be estimated from the intrinsic viscosities determined under non-theta conditions using Equation 2.6 (corrections for the heterodispersity in molecular weight were not made because the samples have similar molecular weight distributions). Figure 3.4 shows that the variation of $[\eta]M^{-\frac{1}{2}}$ with $M^{\frac{1}{2}}$ according to the BSF equation is linear, with the data points for the fully and partially hydrolyzed

TABLE 3.2

UNPERTURBED MOLECULAR DIMENSIONS

SAMPLE	FREELY JOINTED (nm)	CONSTANT BONDANGLE (nm)	EXPERIMENTAL (nm)	STERIC FACTOR
Vinol 107	6.29	8.89	16.71	1.88
Vinol 325	10.78	15.24	28.63	1.88
Vinol 350	12.20	17.25	32.40	1.88
Vinol 205	5.31	7.51	14.77	1.97
Vinol 523	10.07	14.24	28.02	1.97
Vinol 540	10.98	15.52	30.54	1.97

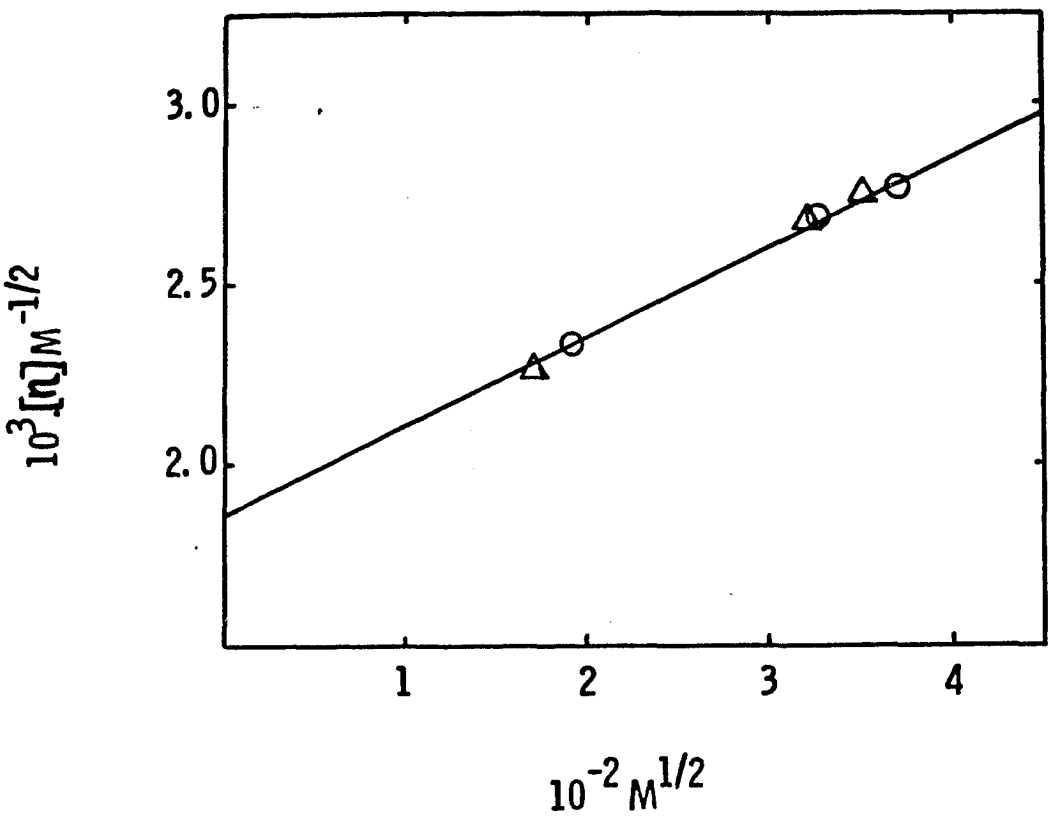

Figure 3.4 Burchard-Stockmayer-Fixman plots: (o) fully hydrolyzed series, (Δ) partially hydrolyzed (88%) series.

polyvinyl alcohols falling on the same line. The intercept of this line gives the value of $K_\theta = 1.8 \times 10^{-3}$ and from the slope the polymer-solvent interaction parameter $\chi = 0.499$ calculated using Equation 2.8, which suggests that water is a poor solvent for polyvinyl alcohol.

Table 3.3 compares the unperturbed and perturbed molecular dimensions. The perturbed coils have expanded dimensions owing to excluded-volume effects and reflect the actual dimensions of a polyvinyl alcohol molecule in solution. The ratio of perturbed to unperturbed dimensions is the expansion factor, the value of which varies from 1.08-1.15 for the various polyvinyl alcohols. The linear viscosity variation combined with the magnitude of the molecular dimensions rule out the presence of aggregates in the dilute aqueous polyvinyl alcohol solutions.

TABLE 3.3

PERTURBED AND UNPERTURBED DIMENSIONS

SAMPLE	UNPERTURBED $(\bar{r}_o^2)^{\frac{1}{2}}$, nm	PERTURBED $(\bar{r}^2)^{\frac{1}{2}}$, nm	$\alpha = (\bar{r}^2/\bar{r}_o^2)^{\frac{1}{2}}$
Vinol 107	16.71	18.03	1.08
Vinol 325	26.63	32.36	1.13
Vinol 350	32.40	37.01	1.14
Vinol 205	14.77	15.92	1.08
Vinol 523	28.02	31.91	1.14
Vinol 540	30.54	35.05	1.15

3.2.3 Transmission Electron Microscopy (TEM)

Obolonkova et al. (82) found globules of 90-110nm diameter in 1% aqueous solutions of fully hydrolyzed polyvinyl alcohol by fracturing the frozen solutions, replicating the fracture surface, and examining the replicas in the transmission electron microscope. They also investigated the effect of time and polyvinyl alcohol concentration. Aging the solutions at room temperature did not affect the size or the degree of aggregation of these globules; however, increasing the polyvinyl alcohol concentration caused the aggregation of the globules into chains to form a network throughout the solution. Similar experiments were carried out in this study using the cold-stage technique in the transmission electron microscope, but no structure formation was observed with either the fully hydrolyzed or the partially hydrolyzed polyvinyl alcohol samples.

3.2.4 Gel Permeation Chromatography (GPC)

Figures 3.5 and 3.6 show the gel permeation chromatograms for the fully and partially hydrolyzed polyvinyl alcohol samples, respectively. The chromatograms comprised single-peaked distributions, indicative of a molecular dispersion of polyvinyl alcohol molecules without aggregates. Double-peaked distributions or single-peaked distributions with a shoulder were observed for some fully hydrolyzed polyvinyl alcohol samples. Figure 3.7 shows that the low-molecular-weight Vinol 107 gave a single-peaked chromato-

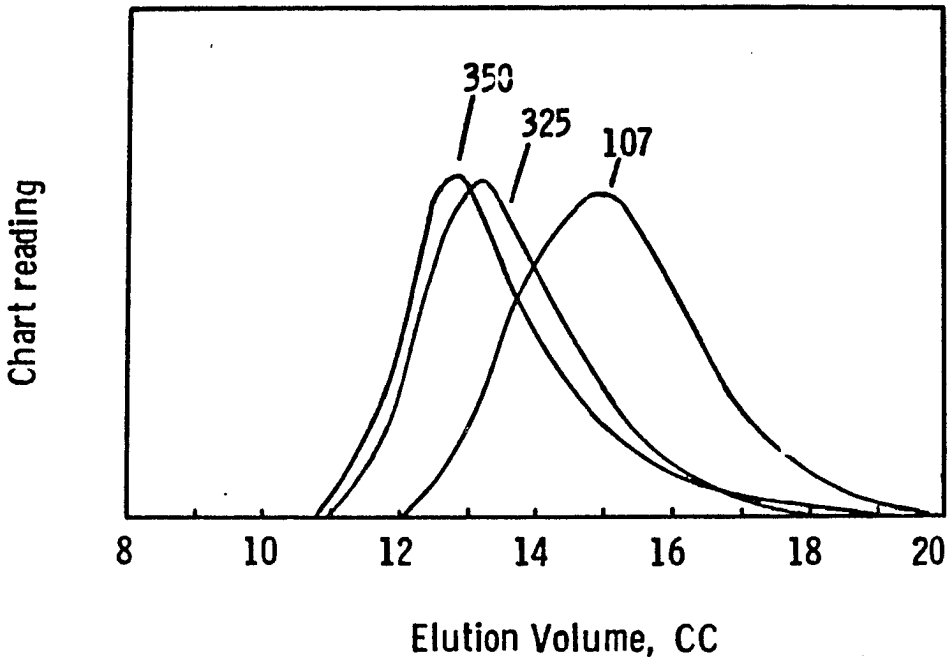

Figure 3.5 Gel permeation chromatograms of the fully hydrolyzed polyvinyl alcohol series. (Concentration of the stock solution: <10% w/v).

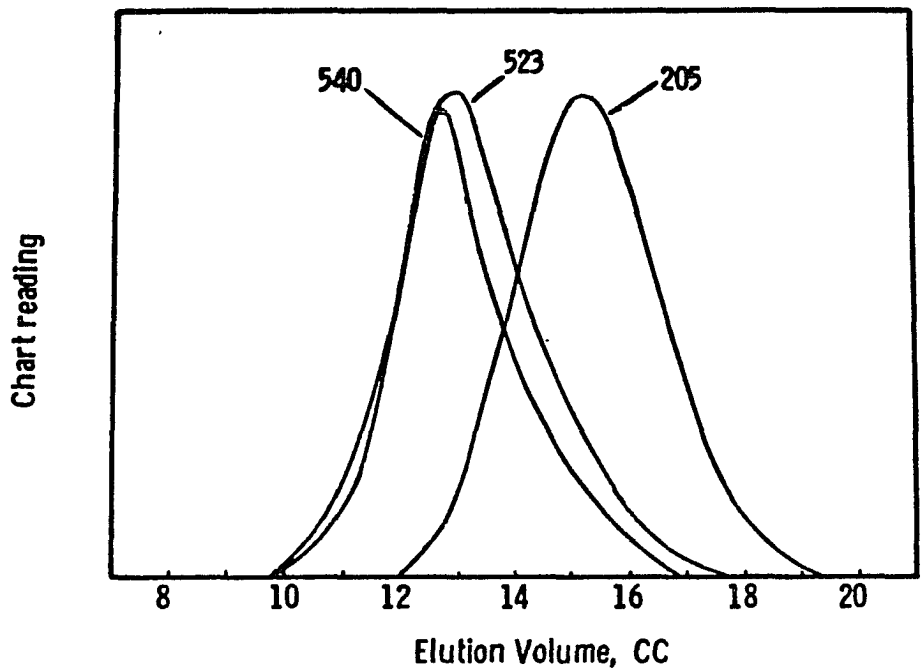

Figure 3.6 Gel permeation chromatograms of the partially hydrolyzed (88%) polyvinyl alcohol series.

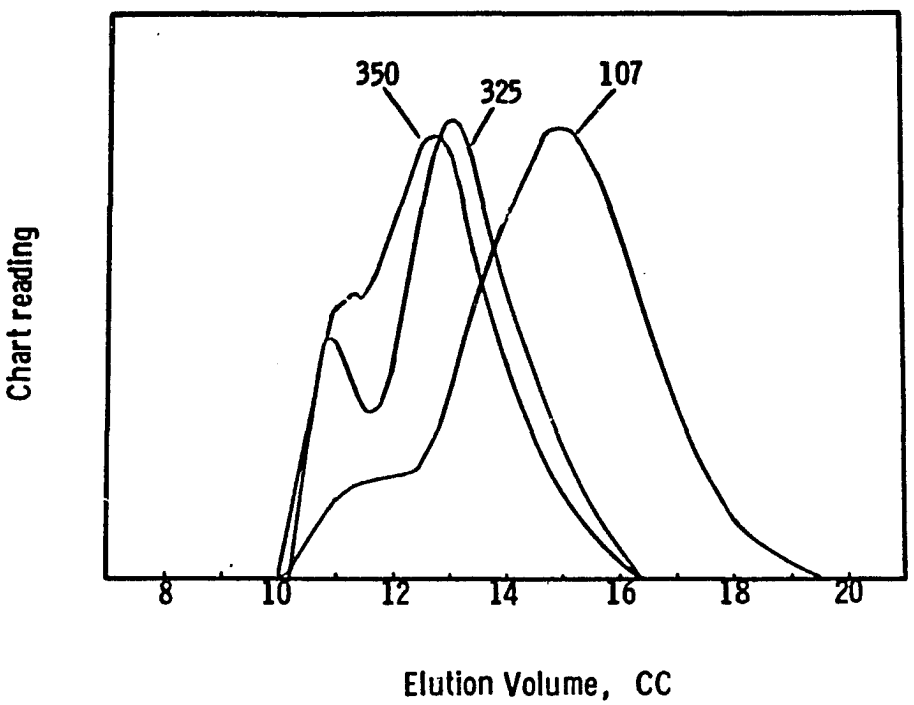

Figure 3.7 Gel permeation chromatograms of the fully hydrolyzed polyvinyl alcohol series. (Concentration of the stock solution: >10% w/v).

gram with a shoulder at low elution volume, and the higher-molecular-weight Vinol 325 and 350 gave distinct double-peaked chromatograms. The peak at high elution volume of the chromatograms in Figure 3.7 coincide well with the peak of the single peak chromatograms in Figure 3.5. The appearance of a second peak or a shoulder at low elution volume was dependent upon the polyvinyl alcohol concentration. When the polyvinyl alcohol solutions were prepared at concentrations of 10% w/v or greater, the second peak was observed even after the solutions were diluted for GPC (but not for solutions prepared at lower concentrations). Since these solutions were heated to dissolve the polyvinyl alcohol, the effect of heating time was investigated, but was found to have no effect on the second peak and hence the degree of aggregation. The aggregation phenomenon observed in concentrated fully hydrolyzed polyvinyl alcohol solutions was not pursued further because the concentrations of the samples prepared for this study were low enough (<<10%) to obviate the aggregation.

3.3 Conclusions

No evidence was found for the association of polyvinyl alcohol molecules in solution arising from intermolecular or intramolecular hydrogen bonding, at least for solutions of low concentration. This was the case for both the fully hydrolyzed and the partially hydrolyzed polyvinyl alcohol solutions. Gel permeation chromatograms showed the presence

of some aggregation, but only in solutions of fully hydrolyzed polyvinyl alcohols prepared at concentrations of 10% or greater, even though these solutions were diluted for GPC. The variation of heating time during solution preparation or after dilution of the concentrated solutions had no effect on the aggregation. The association of polyvinyl alcohol molecules in concentrated solutions was not investigated further because it was not relevant to this work.

4. ADSORPTION OF POLYVINYL ALCOHOL ON POLYSTYRENE LATEX PARTICLES

4.1 Introduction

The adsorption of polyvinyl alcohol (PVA) is important in many practical applications such as textile sizing, adhesion, and coatings. The adsorption of polyvinyl alcohol has also been the subject of studies by many workers. The main contributions have come from two groups: the Dutch group of Fleer, Koopal and others, who studied the adsorption of polyvinyl alcohol on silver iodide particles and the English group of Garvey, Vincent, and Tadros, who studied the adsorption of polyvinyl alcohol on polystyrene latex particles; however, both studies used only a limited polyvinyl alcohol concentration range.

In Chapter 1, it was postulated that a complete characterization of the adsorption behavior requires the determination of five parameters. Of these five parameters, the adsorption density, which is the surface concentration of the polymer at the plateau region of the adsorption isotherm, is the parameter that is most commonly reported. The determination of adsorption isotherms at liquid-solid interfaces involves a mass balance on the amount of polymer added to the dispersion, which requires the separation of the serum from the particles. Centrifugation is often used for this separation, under the assumption that the

adsorption equilibrium does not change during this process. The use of serum replacement (75) allows the separation of the serum from the particles without any assumptions as to the adsorption equilibrium. The system used in this study is similar to that used by the English group (88) with the exception that higher concentrations of polyvinyl alcohol were used. This resulted in some new features which were not recognized in the past. Higher concentrations were used because of their importance in the emulsion polymerization of vinyl acetate, where polyvinyl alcohol is used as emulsifier in concentrations of 4-6% w/v based on water phase. The application of serum replacement led to a thorough analysis of the isotherms by both the adsorption and desorption techniques. Despite the widespread use of polyvinyl alcohol as emulsifier for polyvinyl acetate latexes, polystyrene latexes were chosen as the adsorbent because of their well-characterized surfaces. The system parameters measured were: i) adsorption density; ii) adsorbed layer thickness; iii) heats of adsorption. An attempt was made to measure the fourth parameter, the polymer bound fraction, but it was not possible to estimate the bound fraction because of experimental difficulties. The segmental density distribution was not measured because it required the use of a neutron scattering facility, which was not available. Three system parameters were studied: i) the molecular weight of the polyvinyl alcohol; ii) the degree

of hydrolysis of the polyvinyl alcohol; iii) the particle size of the polystyrene latex.

4.2 Results and Discussion

4.2.1 Serum Replacement of Polyvinyl Alcohol Solutions

Control experiments were carried out to demonstrate that polyvinyl alcohol could be removed from a serum replacement cell by pumping water through the cell. Any adsorbate should be removed according to the equation (75):

$$C_A = C_{Ao} \exp^{-q/V} \qquad 4.1$$

where C_{Ao} is the initial polyvinyl alcohol concentration, C_A the concentration of polyvinyl alcohol in the effluent stream, q the cumulative volume of the effluent stream, and V the volume of the sample placed in the cell. Table 4.1 compares the experimental and theoretical (Equation 4.1) data for the removal of fully hydrolyzed low-molecular-weight polyvinyl alcohol (Vinol 107) using a Nuclepore filtration membrane of 0.2μm pore size. Figure 4.1 shows the variation of $-\ln C_A/C_{Ao}$ with q/V from the data of Table 4.1; the solid line represents the theoretical values. It can be seen that the rate of removal of the polyvinyl alcohol is in good agreement with the theoretical predictions. These control experiments were repeated with other polyvinyl alcohols (Vinol 325 & 350) with equally good agreement between experiment and theory. The use of membranes of pore size smaller than 0.2μm in diameter hindered the

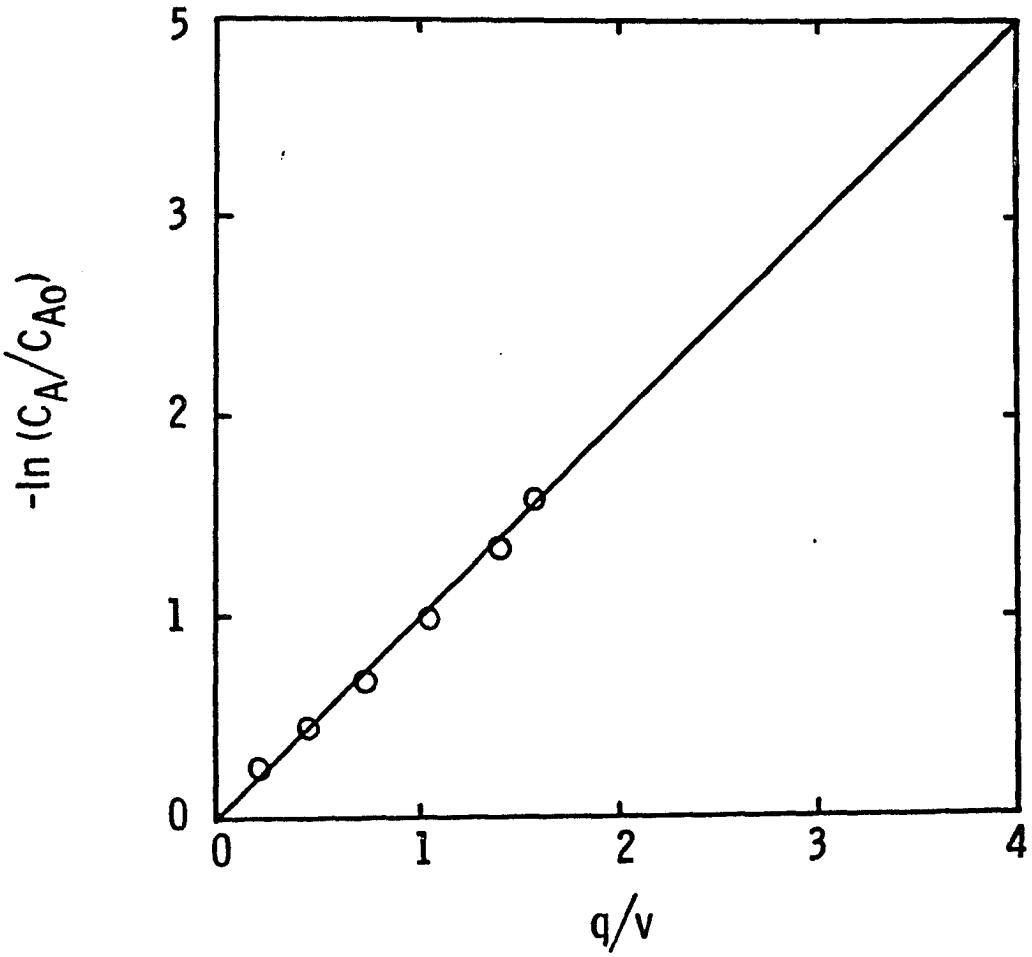

Figure 4.1 Comparison of the experimental and theoretical concentration of polyvinyl alcohol (Vinol 107) in the effluent stream.

TABLE 4.1

COMPARISON OF EXPERIMENTAL AND THEORETICAL CONCENTRATION OF POLYVINYL ALCOHOL IN THE EFFLUENT STREAM

TIME, HRS.	q/V	EXPERIMENTAL C_A,%	THEORETICAL C_A,%
0.00	0.00	----	(2.00)
2.00	0.22	1.57	1.60
4.00	0.46	1.29	1.27
6.35	0.74	1.00	0.95
8.35	1.07	0.74	0.68
10.35	1.42	0.52	0.49
11.35	1.59	0.41	0.41

removal of polyvinyl alcohol, as evidenced by the lower-than-predicted polyvinyl alcohol concentrations in the effluent stream. The flow rate through the serum replacement cell also affected the rate of removal of the polyvinyl alcohol. Flow rates of 10-40 cm^3/hour (cell specification: 11.0 cm in diameter, 21.6 cm in height, and 38.5 cm^2 in filtration area) gave good agreement between experiment and theory; flow rates less than 10 cm^3/hour and greater than 40 cm^3/hour gave experimental polyvinyl alcohol concentrations which were lower and higher, respectively, than predicted by theory.

4.2.2 Effect of Molecular Weight and Degree of Hydrolysis

Figures 4.2 and 4.3 show the adsorption isotherms determined by the adsorption and desorption methods for the

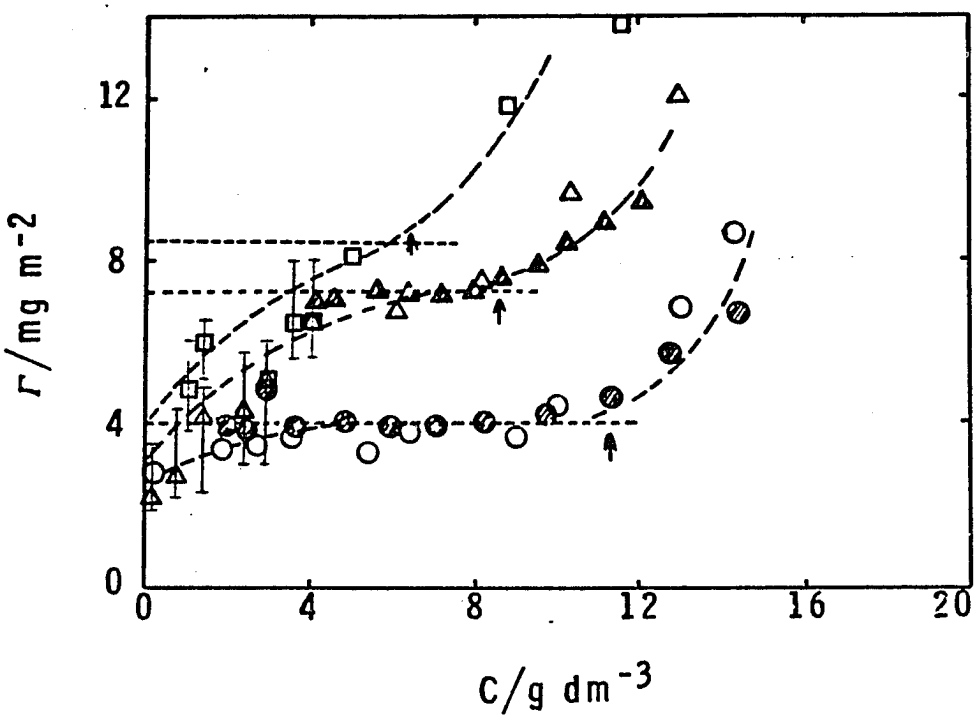

Figure 4.2 Adsorption isotherms of fully hydrolyzed polyvinyl alcohol samples on 190nm polystyrene particles: (o) Vinol 107; (Δ) Vinol 325; (□) Vinol 350; open points by adsorption method and shaded points by desorption method.

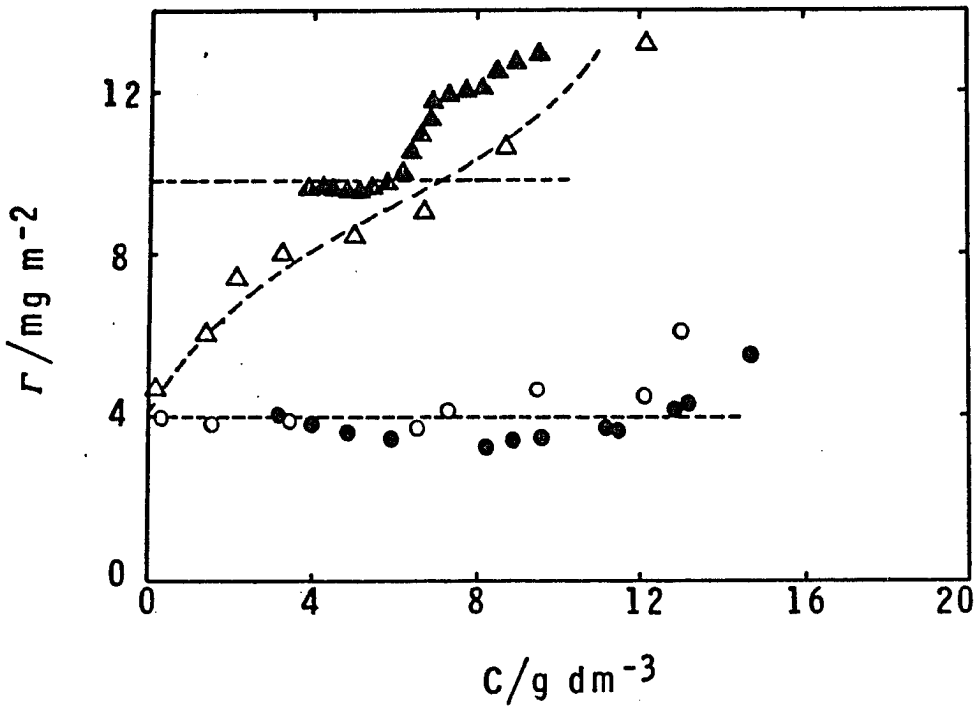

Figure 4.3 Adsorption isotherms of partially hydrolyzed (88%) polyvinyl alcohol samples on 190nm polystyrene particles: (o) Vinol 205; (Δ) Vinol 523; open points by adsorption method and shaded points by desorption method.

fully (98%) and partially (88%) hydrolyzed polyvinyl alcohols, respectively. These isotherms may be analyzed in two ways: by moving from left to right (adsorption) and by moving from right to left (desorption). For the adsorption method, the polyvinyl alcohol surface concentration increased rapidly with increasing bulk polyvinyl alcohol concentration, and then more gradually, to reach a plateau. The gradual increase or rounding of the isotherm was more pronounced with the higher-molecular-weight polyvinyl alcohols. Cohen-Stuart et al. (92) proposed the adjectives "sharp" and "rounded" to describe the inflection points of isotherms obtained with polymer adsorbates of different molecular dispersity; a polymer of narrow molecular weight distribution gave a sharp isotherm, and one of broad molecular weight distribution a rounded isotherm. This nomenclature was applied to the isotherms of Figures 4.2 and 4.3: the low-molecular-weight Vinol 205 (polydispersity 1.3) gave a sharp isotherm; all other polyvinyl alcohols (polydispersities ca. 1.5) gave rounded isotherms, with the degree of rounding being more pronounced with the high-molecular-weight polyvinyl alcohols. Figure 4.2 shows scattered data points in the low bulk polyvinyl alcohol concentration range for the high-molecular-weight fully-hydrolyzed Vinol 325 and Vinol 350. This scatter may be explained by the "bridging" flocculation postulated for partial coverage of the particles by the polymer adsorbates: a single polymer molecule

adsorbed on two or more particles simultaneously. In this case, the surface polymer concentration would be lower than in the absence of bridging, which would affect the shape of the adsorption isotherm. The scatter observed for Vinol 325 and Vinol 350 is in the region of partial coverage. The method of mixing the polymer with the colloidal sol affects the flocculation by bridging; however, adding the polyvinyl alcohol solution to the latex or vice-versa gave no difference in the shape of the adsorption isotherm.

Hydrodynamic chromatography and photon correlation spectroscopy were used to detect these flocs. Hydrodynamic chromatography showed no evidence of the presence of flocs; however, in this method, the particles are subjected to shear rates of 600-1000 sec^{-1}, which may break the flocs down to primary particles. Photon correlation spectroscopy showed that the particle size increased to twice the bare particle size at partial coverage and then decreased to a size which was still larger than that of the bare particles at the plateau region. Table 4.2 gives the particle size variations for Vinol 350 adsorbed on the 190nm-size particles. The larger particle sizes observed at partial coverage are consistent with flocculation by bridging. The smaller particle sizes observed at the plateau region are consistent with the absence of flocculation at full surface coverage. The increase in size (48nm) at the plateau region relative to that of the bare particles is a measure

TABLE 4.2

PARTICLE SIZE AND δ AS A FUNCTION OF SURFACE COVERAGE FOR THE 190nm-VINOL-350 SAMPLES BY PHOTON CORRELATION SPECTROSCOPY

DESCRIPTION	PARTICLE SIZE (nm)	δ (nm)
Bare particle	180±4.5	---
Increasing surface coverage but below the apparent plateau region of the isotherm	295±5.7	---
	307±13.0	---
	313±3.9	---
	363±12.1	---
At or slightly above the plateau adsorption	276±4.0	48±3.3

of the thickness (δ) of the adsorbed polyvinyl alcohol layer. Transmission electron microscopy also gave evidence for flocculation by bridging at partial coverage. Figure 4.4 shows electron micrographs of the bare particles and the particles covered partially with adsorbed Vinol 350. The partially covered particles were interconnected with fibrillar links, which were not observed in the bare-particle sample. These results confirm the existence of weak or labile flocs at partial coverage, particularly with the high-molecular-weight fully-hydrolyzed Vinol 325 and Vinol 350. In contrast, the partially-hydrolyzed Vinol 523, which is comparable in molecular weight to the Vinol 325, gave an adsorption isotherm with little scatter, indicating the absence of flocculation. Partially hydrolyzed polyvinyl alcohol shows specific interactions with polystyrene surfaces (mentioned below), and the absence of flocculation in this case is consistent with the theory proposed by

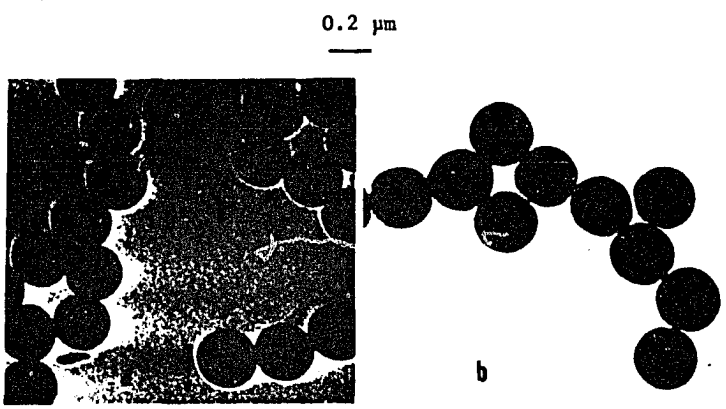

Figure 4.4 Transmission electron micrographs of 190nm polystyrene latex: (a) without PVA (b) with Vinol 350 at partial coverage.

Clark and Lal (93) for flocculation by bridging. Table 4.3 shows that the adsorption densities at the plateau region increase with increasing polyvinyl alcohol molecular weight, despite the distribution of molecular weights for each sample. The adsorption density of Vinol 350 is given in parentheses because of the difficulty in establishing its exact value. For the fully hydrolyzed polyvinyl alcohols, which show no specific interactions with polystyrene surfaces, the increase in adsorption density was proportional to the 0.5 power of the molecular weight, in good agreement with the predicted proportionality to the square root of the molecular weight for weak surface interactions under theta conditions. For the partially hydrolyzed polyvinyl alcohols, which show specific interactions with polystyrene surfaces, the increase in adsorption density is proportional to the 0.72 power of the molecular weight. For comparable molecular weights, Garvey (88) found adsorption densities of

TABLE 4.3

ADSORPTION DENSITY AT THE APPARENT PLATEAU FOR THE DIFFERENT PVA'S

SAMPLE	$\Gamma/(mg\ m^{-2})$	REPEAT UNITS/100$\AA^2$
Vinol 107	4.00	55
Vinol 325	7.20	98
Vinol 350	(8.50)	(116)
Vinol 205	4.00	49
Vinol 523	9.86	121

fractionated 88%-hydrolyzed polyvinyl alcohol on polystyrene latex particles that were only one-half of those reported here; the adsorption densities increased with the 0.5 power of the molecular weight. These results were stated to be in good agreement with theory, even though the 88%-hydrolyzed polyvinyl alcohols show specific interactions with polystyrene surfaces. For the same system, Boomgaard et al. (94) found adsorption densities 50-100% greater than those found by Garvey and attributed the difference to the different polystyrene surfaces in the two works.

On adsorption, partially hydrolyzed polyvinyl alcohol shows specific interactions with the substrate: the more hydrophobic acetyl groups adsorb preferentially on hydrophobic polystyrene surfaces. Partially hydrolyzed polyvinyl alcohol is a better stabilizer than fully hydrolyzed polyvinyl alcohol because of its increased degree of blockiness of the acetyl units. The 88%-hydrolyzed polyvinyl alcohol samples used in this study have mean acetyl runlengths of three units. Consequently, the adsorption densities of partially hydrolyzed polyvinyl alcohols of comparable molecular weights should be higher than those of the fully hydrolyzed polyvinyl alcohols. This was the case for Vinol 523, which has a molecular weight comparable to that of Vinol 325; however, the adsorption densities of the fully hydrolyzed Vinol 107 and partially hydrolyzed Vinol 205 were the same, even though the molecular weight

of Vinol 205 was slightly lower than that of Vinol 107. The molecular weight of partially hydrolyzed polyvinyl alcohol would be higher than that of the fully hydrolyzed analog if both were prepared by hydrolysis of the same polyvinyl acetate. Since Vinol 205 also has a narrower molecular weight distribution than Vinol 107, it may have been made from a different polyvinyl acetate and therefore may not be suitable for comparison.

Extension of the adsorption isotherms to higher bulk polyvinyl alcohol concentrations gave a second rise in surface concentration due to multilayer adsorption. Silberberg (21) explained multilayer adsorption in terms of an incipient phase separation at the surface. The phase separation process should be concentration-dependent; since the surface concentration is usually higher than the bulk concentration and increases with increasing molecular weight, phase separation should occur at lower concentrations for the higher-molecular-weight polyvinyl alcohols. Figures 4.2 and 4.3 show that this second rise occurs at a lower bulk concentration for the higher-molecular-weight polyvinyl alcohols. Extension of the isotherms to still higher bulk concentrations was not possible because the differential refractometer was limited in the concentration range it could measure. For the desorption method (moving from right to left), the isotherms can be divided into two regions: (i) a region where the surface concentration decreases upon

moving to the left; (ii) a region in which the surface concentration remains unchanged. The fact that polymer adsorbed in the multilayer region can desorb indicates that the polymer coil had no attachment to the surface, as postulated by Silberberg (21). Gel permeation chromatography of the desorbed fractions showed the same molecular weight distribution as the original polyvinyl alcohol, indicating that the adsorption was not preferential with respect to molecular weight; however, these desorbed fractions were from a region of saturation or near-saturation adsorption. Preferential adsorption of higher molecular weight polymers is important in the rounded part of the isotherm (discussed earlier); however, the fact that the same distribution was restored upon saturation shows the transitory nature of this phenomenon. Also, the gel permeation chromatograms showed no evidence of aggregation, whereas the occurrence of phase separation suggests the formation of aggregates. It may be argued that gel permeation chromatography requires extreme dilution of the samples and that any aggregates that may have existed would disperse upon dilution; however, it has been shown (Section 3.2.4; reference 95) that, for these polyvinyl alcohols, gel permeation chromatography distinguished aggregates which were not dispersed upon dilution. The second region in which the surface concentration remained unchanged indicates that the adsorption was irreversible; however, the concentrations used may have been too

low and the times too long for any desorption to be observed, as proposed by Scheutjens et al. (27). Comparison of the isotherms determined by adsorption and desorption shows good agreement for the low-molecular-weight polyvinyl alcohols. For Vinol 350, it was not possible to determine the isotherm by desorption because of an irregular decay in concentration upon desorption. With Vinol 523, the agreement in the multilayer adsorption region was poor. Nonetheless, the desorption isotherms gave well-defined plateau values, which was not the case for the adsorption isotherms.

4.2.3. Effect of Molecular Weight and Degree of Hydrolysis on Adsorbed Layer Thickness

Figure 4.5 shows the variation of reduced specific viscosity with volume fraction for the bare and PVA-covered 190nm-size polystyrene latex particles. For the bare particles, η_{red}/ϕ was independent of ϕ and the value of the Einstein coefficient was ca. 3.0. For the PVA-covered particles, η_{red}/ϕ increased linearly with ϕ. Table 4.4 gives the adsorbed layer thicknesses calculated from the differences in the intercepts of the extrapolated η_{red}/ϕ-ϕ plots for the bare and PVA-covered particles and determined by photon correlation spectroscopy, as well as the root-mean-square radii of gyration of the free polymer coil in solution. The agreement of the adsorbed layer thicknesses determined by two independent methods is remarkable. The

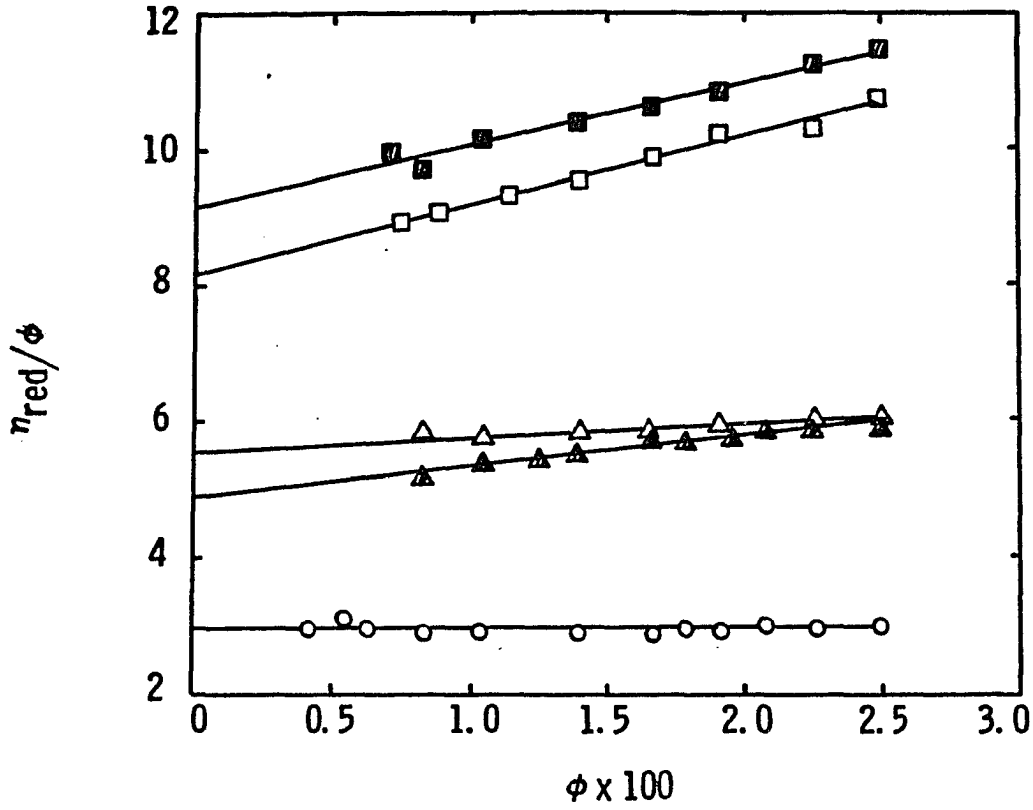

Figure 4.5 Reduced viscosity ratio versus volume fraction of 190nm polystyrene particles: (o) bare particles, (Δ) covered with Vinol 107; (□) covered with Vinol 325; (▲) covered with Vinol 205; (▣) covered with Vinol 523.

increase in adsorbed layer thickness followed the same dependence on molecular weight as the adsorption density, i. e., δ was proportional to the 0.5 power of the molecular weight for the fully hydrolyzed polyvinyl alcohols and

TABLE 4.4

ADSORBED LAYER THICKNESS δ AND THE RMS RADIUS OF GYRATION $(\bar{S}^2)^{\frac{1}{2}}$

SAMPLE	δ BY VISCOSITY, nm	δ BY PCS, nm	$(\bar{S}^2)^{\frac{1}{2}}$, nm	$\delta/2(\bar{S}^2)^{\frac{1}{2}}$
190nm PS-107	22.0±2.0	25.0±2.0	7.4	1.48-1.69
190nm PS-325	37.9±2.0	39.9±2.5	13.2	1.44-1.51
190nm PS-350	---	48.2±4.3	15.1	1.60
190nm PS-205	17.4±2.0	16.0±2.0	6.5	1.23-1.34
190nm PS-523	43.0±2.0	45.5±3.5	13.0	1.65-1.75

to the 0.72 power for the partially hydrolyzed polyvinyl alcohols. Viscometric measurements were not made for Vinol 350 because of the aforementioned problems in generating the desorption isotherms; the value for the adsorbed layer thickness at the saturation region of the adsorption isotherm measured by photon correlation spectroscopy was taken from Table 4.2. The adsorbed layer thicknesses were 40-70% greater than the dimensions of the polymer coil in solution (assuming that the thickness of the coil adsorbed at the surface is twice the radius of gyration) except for Vinol 205, indicating that the polymer coil became distorted or elongated normal to the surface upon adsorption.

4.2.4 Effect of Molecular Weight and Degree of Hydrolysis on Heats of Adsorption

Figure 4.6 shows that the variation of heat of adsorption with time for the fully hydrolyzed Vinol 107 and Vinol 325, and the partially hydrolyzed Vinol 523, on the 190nm-size polystyrene latex particles over the normal period of 15 minutes was irregular initially and then became linear. The initial irregular patterns were artifacts resulting from the extreme sensitivity of the instrument. Therefore, the data for the first five minutes were omitted from the heat computations. The linear region of the heat curve was an indication that the heat evolution was incomplete in the time allowed for adsorption. Table 4.5 gives the heats of adsorption calculated from the difference in the values at 5 and 15 minutes for the various polyvinyl alcohol samples; the heats evolved over a period of 15 minutes were small and did not show any trend. The heats evolved for the first two cases were about the same for different molecular weights. This result is not unexpected because the heat evolution is independent of molecular weight. With polyvinyl alcohols of the lower degree of hydrolysis and the same molecular weight, the polymer-surface interaction would be greater and therefore higher heats of adsorption would be expected with the partially hydrolyzed polyvinyl alcohols. On the contrary, the 88%-hydrolyzed Vinol 523, which was comparable in molecular weight to the fully hydrolyzed

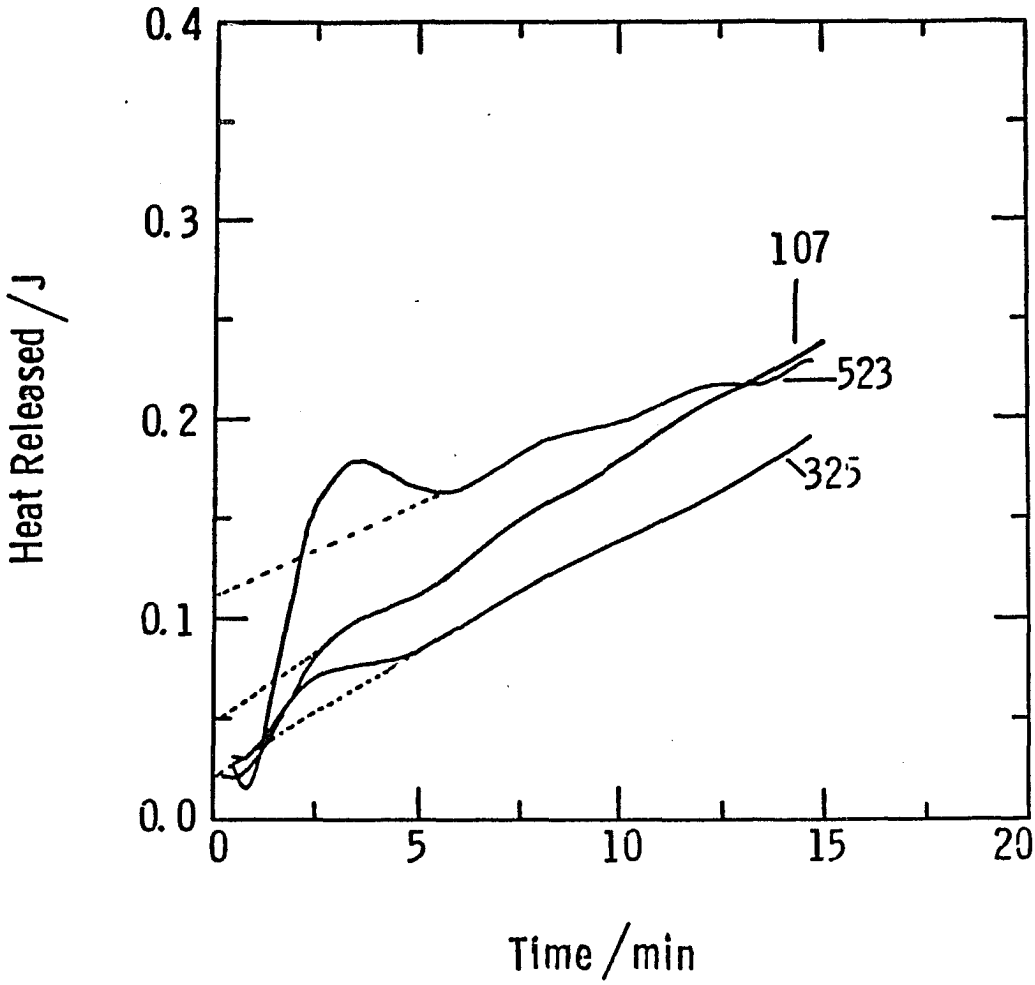

Figure 4.6 Heat of adsorption as a function of time for different polyvinyl alcohol samples on 190nm polystyrene particles (15 minutes run).

TABLE 4.5

SAMPLE SPECIFICATION AND HEATS OF ADSORPTION OF PVA ON 190 nm PS PARTICLES FOR A 15 MINUTE EXPERIMENTAL RUN

SAMPLE	% HYDROLYSIS	$\bar{M}w$	$-\Delta H$ (J/m^2)
Vinol 107	98	35,800	0.0168
Vinol 325	98	118,100	0.0140
Vinol 523	88	120,400	0.0085

Vinol 325, gave lower heats of adsorption. Measurement of the polyvinyl alcohol surface concentration of the samples gave values only 10-25% of the saturation adsorption, demonstrating that 15 minutes was too short a time for the adsorption to reach equilibrium. Therefore, the experiments were carried out over a period of 15 hours (900 minutes) instead of the normal 15 minutes to provide enough time for the adsorption to reach its saturation value. Figure 4.7 shows that times of about 800 minutes were required for the heat of adsorption curves to reach equilibrium and that there were significant differences in the heat curves for the various polyvinyl alcohols. Table 4.6 shows that the heats of adsorption measured during the 900-minute runs were 25-95 times greater than those generated during the normal 15-minute runs. The evolution of heat on the adsorption of polymer molecules at the liquid-solid interface comes from two sources: i) polymer-surface interactions; ii) polymer-polymer interactions. The polymer-surface interactions depend upon the number of contacts of

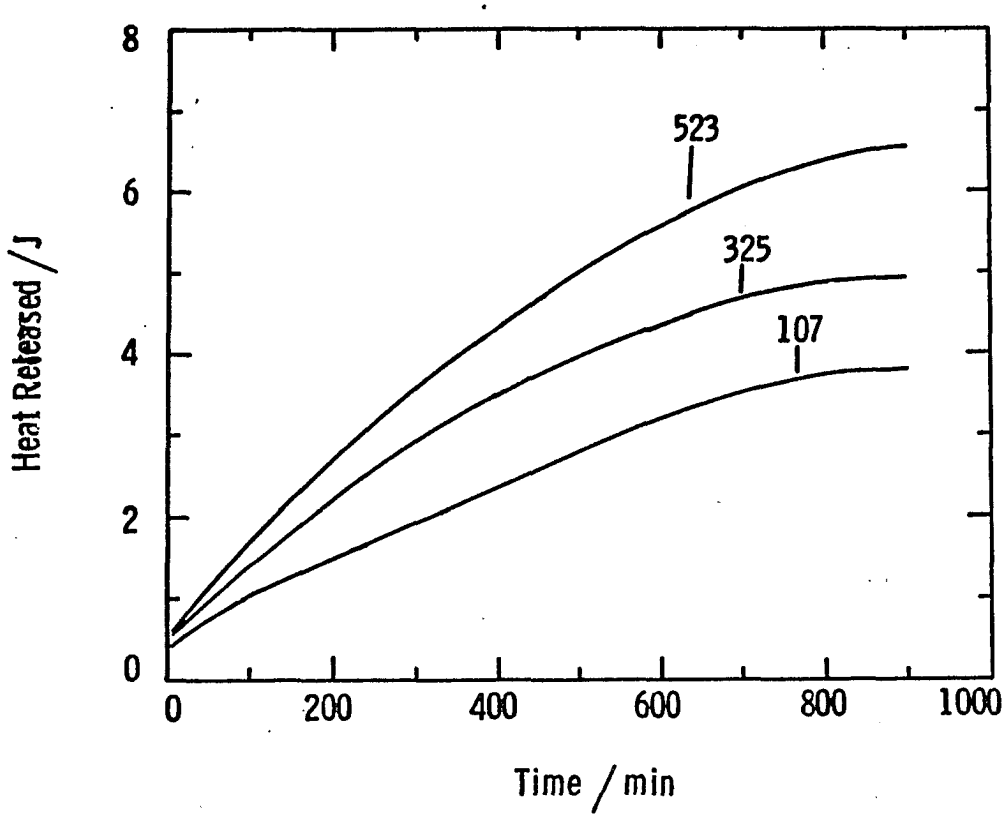

Figure 4.7 Heat of adsorption as a function of time for different polyvinyl alcohol samples on 190nm polystyrene particles (15 hours run).

the polymer coil with the surface, which result from the breaking of solvent-surface and solvent-polymer contacts and the formation of polymer-surface and solvent-solvent contacts; their contribution to the heat of adsorption is designated as ΔH_{tr}. With the hydrophobic polystyrene surface, the solvent-surface interactions are negligible. It is not necessary that the solvent molecules become detached from the polymer coil for adsorption to take place. For the polystyrene-nonionic polymer system, the heat contribution is expected from the relatively weak hydrophobic

TABLE 4.6

COMPARISON OF HEATS OF ADSORPTION OF PVA ON 190nm PS PARTICLES FOR DIFFERENT EXPERIMENTAL TIMES

SAMPLE	% HYDROLYSIS	$\bar{M}_w$	$-\Delta H (J/m^2)$ (15 min run)	$-\Delta H (J/m^2)$ (900 min run)
Vinol 107	98	35,800	0.0168	0.4377
Vinol 325	98	118,100	0.0140	0.5567
Vinol 523	88	120,400	0.0085	0.7995

polystyrene-polymer interactions and the replacement of polymer-solvent contacts in the adsorbed layer by polymer-polymer contacts. These contributions are designated as ΔH_{tr} and ΔH_{mix} respectively. Therefore, the total heat of adsorption is given by:

$$\Delta H_{ads} = \Delta H_{tr} + \Delta H_{mix} \qquad 4.2$$

The contribution of the ΔH_{mix} term to the total heat of adsorption is negligible (96) except where the heat of adsorp-

tion depends upon the molecular weight of the polymer. The heat of hydrophobic interactions between polystyrene and polyvinyl alcohol is of the order of 5-30 mJ/m^2, as estimated from the decrease in surface tension of water with polyvinyl alcohols. Table 4.6 shows that the heats of adsorption were considerably higher than expected if the ΔH_{tr} term was the greatest contribution to the heat of adsorption. Also, the values of the ΔH_{ads} term increased with increasing polyvinyl alcohol molecular weight. The higher heats of adsorption and the dependence of the ΔH_{ads} on molecular weight suggests that the contribution of the ΔH_{mix} term is not only significant but is dominant. The χ value of 0.499 calculated from the intrinsic viscosity measurements (Sect. 3.2.2) indicates that the interactions between polyvinyl alcohol molecules and water are weak and the segmental interactions within the polymer coil are strong. On adsorption at the liquid-solid interface, the polymer coil loses its compact configuration, and it is possible that there are stronger interactions between the extended loops at the interface and water. These polymer-solvent interactions result from hydrogen bonding, (heats of the order of 5 Kcal/mole are liberated from hydrogen bonding) which can account for the higher heats of adsorption as well as the trends observed with increasing molecular weight and decreasing degree of hydrolysis. It should be emphasized that the functional groups of the ex-

tended loops of the adsorbed partially hydrolyzed polyvinyl alcohol molecules are identical to those of the fully hydrolyzed polyvinyl molecules because of the preferential adsorption of the acetyl groups. Therefore, it is not surprising that the heats of adsorption of the thicker films of the 88%-hydrolyzed polyvinyl alcohol are higher. This explanation is in contrast to the earlier postulation that the contribution of the ΔH_{mix} term to the heat of adsorption was generally negligible and that, when it was significant, it originated from the replacement of the polymer-solvent contacts by the polymer-polymer contacts in the adsorbed layer. For polyvinyl alcohol, the polymer-polymer contacts of the coil in solution are strong, and adsorption is favored by strong polymer-solvent interactions in the adsorbed layer.

4.2.5 Effect of Latex Particle Size on Adsorption

Figure 4.8 shows the adsorption isotherms of Vinol 107 on polystyrene latex particles of 190, 400, and 1100nm diameter. The different-size latex particles give the same type of isotherm, and the adsorption densities at the plateau region are independent of particle size. It should be mentioned that, for these studies of different particle size, the concentration of polymer added must be adjusted so that the amount of polymer per unit surface area must be about the same for the different-size particles; the polymer concentration suitable for the smaller particles

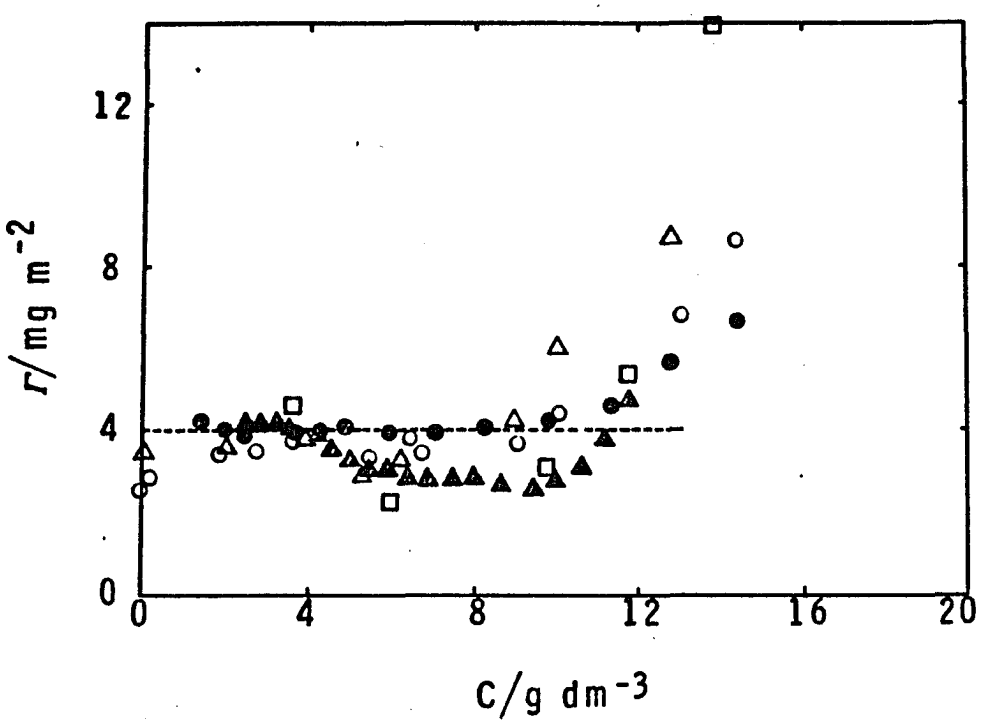

Figure 4.8 Adsorption isotherms of Vinol 107 on different size polystyrene particles: (o) 190nm particles; (Δ) 400nm particles; (□) 1100nm particles; open points by adsorption method and shaded points by desorption method.

may be too great for the larger particles, which would give an isotherm with a higher plateau region. This aberration was observed in a desorption experiment with the 400nm-size particles, perhaps because of the adsorption of polymer aggregates, which are present in concentrated polyvinyl alcohol solutions. Comparison of the desorption isotherms of Figure 4.8 show that the data points for the 400nm-size particles fall at a lower surface concentration in the higher bulk concentration region and do not match the isotherm determined by adsorption. The data points on 1100nm particles are limited because of the limited amount of sample that was available.

4.2.6 Effect of Latex Particle Size on Adsorbed Layer Thickness

Figure 4.9 shows that the variation of reduced specific viscosity with volume fraction for the 190, 400, and 1100nm-size bare polystyrene latex particles was the same; the Einstein coefficient was ca. 3.0. The variation of reduced specific viscosity with concentration for the different-size PVA-covered particles was linear, with the same slopes but different intercepts. Table 4.7 gives the adsorbed layer thicknesses calculated from the viscosity measurements and determined by photon correlation spectroscopy. The adsorbed layer thickness for the 1100nm-size particles could not be measured by photon correlation spectroscopy, which is limited to particle sizes of 1000nm or smaller. Again, the agreement between the two methods

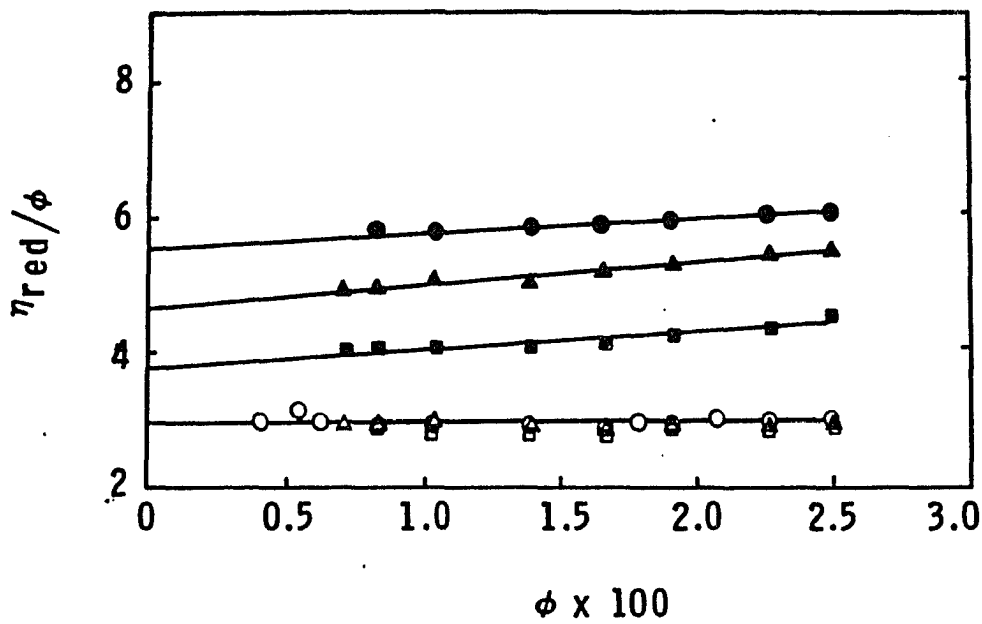

Figure 4.9 Reduced viscosity ratio versus volume fraction of polystyrene particles of different sizes: (o) 190nm particles; (Δ) 400nm particles, (□) 1100nm particles; open points for bare particles and closed points for covered particles.

was excellent. The absorbed layer thickness increased with increasing latex particle size, proportionally to the 0.5 power of the particle radius R. This relationship holds for the 190-1100nm range studied; however, there are limits to its applicability in terms of adsorbed layer thickness and latex particle size. Garvey (88) experienced difficulty in measuring the adsorbed layer thickness of 165 nm-size polystyrene latex particles by ultracentrifugation and therefore used the smaller 38nm-size particles for these measurements; however, he also experienced difficulty in measuring the adsorption isotherm of the latter latex and therefore made the assumption that the adsorption per unit area was the same for both latexes, and compared the adsorbed layer thicknesses obtained for the 165nm-size latex by photon correlation spectroscopy with the values obtained for the 38nm-size latex by ultracentrifugation. The adsorbed layer thicknesses of various polyvinyl alcohols on the 38nm-size latex particles measured by ultracentrifugation were smaller than those on the 165nm-size latex particles measured by photon correlation spectroscopy. Garvey attributed this difference to the different particle sizes of the latexes and made the following assumptions to account for this difference: (i) the adsorbed layer on different-size particles is homogeneous with respect to segment density; (ii) the adsorbed layers occupy a constant volume per unit surface area on different-size particles.

He then defined the effective flat surface thickness δ_{eff} as the ratio of the total volume of the adsorbed layer to the surface area of the particle. The implication of this work is that the increase in adsorbed layer thickness observed with the larger particles is due only to the geometry of the system. It will be shown below that, for different-size particles, the term δ_{eff} has no significance and that the assumption of constant volume of the adsorbed layer is inappropriate. Table 4.7 shows that the values of δ_{eff} calculated according to Garvey's procedure increased with increasing particle size.

TABLE 4.7

ADSORBED LAYER THICKNESS δ AND THE EFFECTIVE FLAT LAYER THICKNESS δ_{eff}

SAMPLE	δ BY VISCOSITY,nm	δ BY PCS,nm	δ_{eff},nm
190nm PS-107	22.0 ± 2.0	25.0 ± 2.0	27.9-32.2
400nm PS-107	32.7 ± 2.0	33.6 ± 3.5	38.3-39.6
1100nm PS-107	54.4 ± 2.0	---	59.9

Therefore, the following explanation is proposed for the increase in the adsorbed layer thickness with increasing latex particle size: (i) the same adsorption density per unit surface area for the different-size particles could result from a decrease in the number of loops, so that the average loops on the larger particles are longer and broader; (ii) it could result from train segments being desorbed to form loops, so that the average loops on the

larger particles are longer and broader; (iii) it could result from both of the foregoing explanations. These explanations suggest that the adsorption on the larger particles is relatively weak, which could be readily established. The lower limit of the adsorbed layer thickness can be defined as about twice the radius of gyration of the polyvinyl alcohol molecules for particles of the appropriate size. This particle size can be calculated from the radius of gyration and the proportionality of the adsorbed layer thickness to the square root of the particle radius. The adsorbed layer thickness increased with increasing latex particle size, and the measured thicknesses were always greater than twice the radius of gyration, the difference increasing with increasing particle size. The upper limit, however, cannot be defined.

4.2.7 Effect of Latex Particle Size on Heats of Adsorption

Figure 4.10 shows the variation of the heat of adsorption with time for Vinol 107 polyvinyl alcohol adsorbed on polystyrene latex particles of 190, 400, and 1100nm diameter. Table 4.8 gives the heats of adsorption calculated from the curves of Figure 4.10. The heats of adsorption on the larger particles are lower. Section 4.2.6 showed that the adsorbed layer thickness increased with increasing latex particle size even though the adsorption densities were identical, and it was postulated that longer and broader, and perhaps fewer, loops were formed on larger particles.

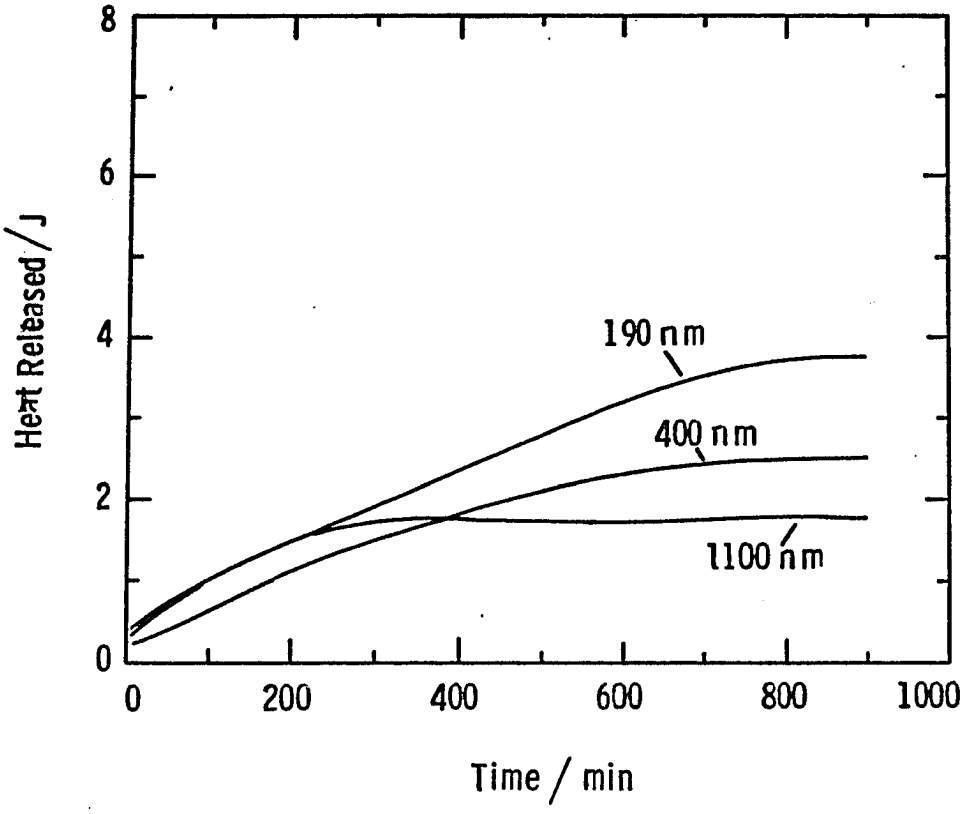

Figure 4.10 Heat of adsorption of Vinol 107 as a function of time for different size polystyrene latex particles.

This would lead to a decrease in the number of segments that are in contact with the surface (weaker adsorption) so that lower heats of adsorption would be expected on larger particles; however, Section 4.2.4 showed that the contribution of the polymer-solvent interactions to the heat of adsorption outweighed the contribution of the polymer-surface interactions. Therefore, the decrease in the number of segments in contact with the surface with increasing particle size may not be perceived in the measurements of the heats of adsorption.

TABLE 4.8

HEATS OF ADSORPTION OF VINOL 107 ON PS PARTICLES OF DIFFERENT SIZES

PARTICLE SIZE (nm)	$-\Delta H$ (J/m^2)
190	0.4377
400	0.3223
1100	0.2717

The question of why the heats of adsorption are lower on larger latex particles must be addressed. The curvature of the surface appears to affect the configuration of the adsorbed polymer coil. Therefore, the enthalpic and entropic effects must both be considered. It was shown earlier that the 0.499 value of χ for the polyvinyl alcohol-water system indicated strong segmental interactions within the polymer coil in solution. The adsorption on larger particles was postulated to be weaker, with longer and broader

loops extending into the medium; therefore, it is conceivable that the configuration of the segments in the loops is closer to that in the free coil, which results in weak polymer-solvent interactions. This can lead to lower heats of adsorption on the larger latex particles. Figure 4.11 shows that the variation of the heat of adsorption with reciprocal latex particle diameter is linear. Extrapolation of this line to zero reciprocal particle diameter shows that the heat that would be liberated from a flat surface is about 0.23 J/m^2. Another interesting feature of the heats of adsorption plots is the dependence of the equilibrium heat values on the latex particle size. Equilibrium is attained in shorter times with the larger particles, which suggests that the adsorption is a diffusion-controlled process governed by dispersion forces.

4.2.8 Polymer Bound Fraction

Various techniques have been used to measure the polymer bound fraction, e.g., spectroscopic techniques such as infrared (IR), nuclear magnetic resonance (NMR), electron spin resonance (ESR) spectroscopy, and microcalorimetry. Each of these techniques has advantages and disadvantages. Infrared spectroscopy depends upon the specific interactions between the functional groups of the polymer and the surface. Nuclear magnetic resonance and electron spin resonance spectroscopy depend upon the differing mobilities of the segments in the loops and the trains;

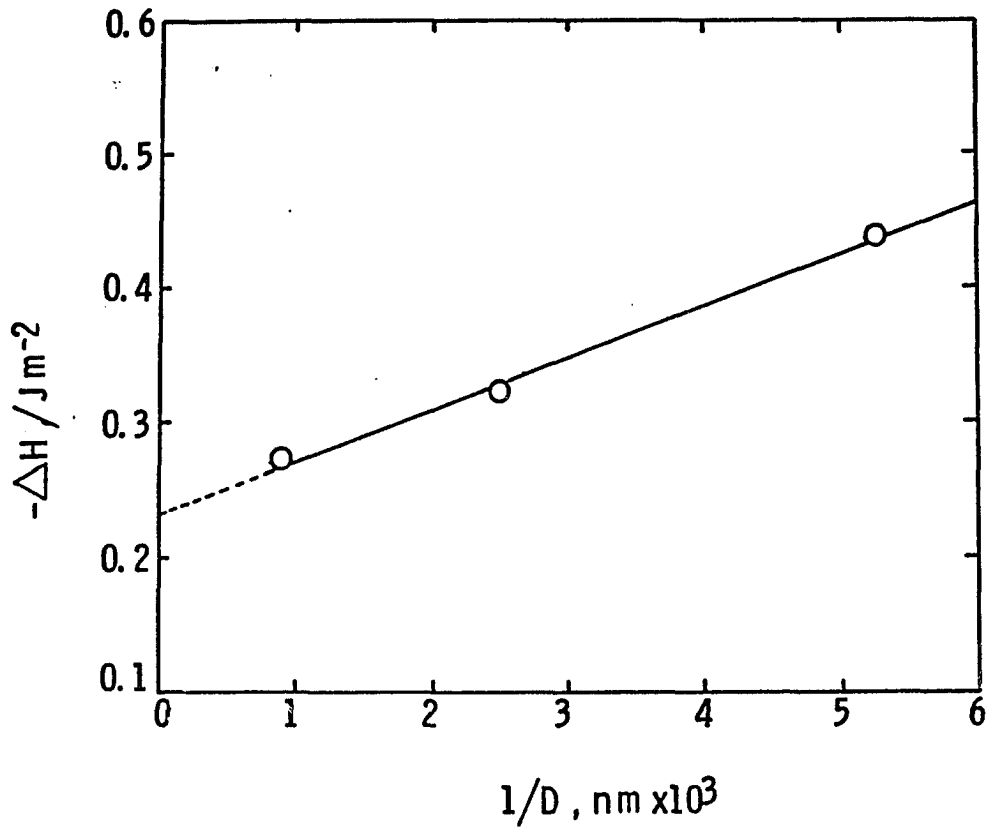

Figure 4.11 Heat of adsorption versus reciprocal diameter of polystyrene particles.

moreover, electron spin resonance spectroscopy requires the attachment of a suitable spin-label. For the polystyrene-polyvinyl alcohol system, nuclear magnetic resonance spectroscopy is probably the most suitable method, except that it requires the use of deuterated polystyrene latex particles. None of these techniques were used because of the foregoing requirements; however, an attempt was made to estimate the bound polymer fraction from the heat of adsorption measured by microcalorimetry. The heat of adsorption of ethanol (which is equivalent in structure to a polyvinyl alcohol segment) was measured for comparison with the heats of adsorption of polyvinyl alcohol. Calculation of the polymer bound fraction from this comparison gave meaningless results (high bound fraction values-about 0.6 with Vinol 107 on 190nm PS particles). Clearly, polymer systems are too complicated to treat rigorously by molecular mechanics. Therefore, microcalorimetry is not a suitable technique to estimate the polymer bound fraction.

4.2.9 Desorption of Polyvinyl Alcohol from Polystyrene Particles

Desorption experiments can provide valuable information about the configuration and energetics of the adsorbed polymer molecules. The desorption of polymer molecules, however, is difficult to accomplish. An attempt was made to desorb the fully hydrolyzed low-molecular-weight Vinol

107 from the 190nm-diameter polystyrene latex particle surface. Section 3.2.2 showed that water is a poor solvent for polyvinyl alcohol. Therefore, any attempt to desorb polyvinyl alcohol must result from an improvement in the solvent power of water. Water-miscible organic solvents, such as acetone, lower alcohols, dioxane, tetrahydrofuran, etc., can be added to aqueous solutions of polyvinyl alcohol without precipitation of the polymer or formation of two phases. Some of these solvents shrink the dimensions of the polyvinyl alcohol molecules in solution, as shown by viscosity measurements (97). Aqueous polyvinyl alcohol solutions are also known to be sensitive to the addition of various electrolytes. Saito (98) investigated the effect of these electrolytes on the configuration of polyvinyl alcohol molecules in aqueous solution. Low concentrations of such electrolytes as potassium and sodium thiocyanates increased the intrinsic viscosity of aqueous polyvinyl alcohol solutions, which indicates that water containing these electrolytes is a better solvent for polyvinyl alcohol than pure water; however, these electrolyte solutions could not be used to desorb polyvinyl alcohol using serum replacement because of their contribution to differential refractive index of the effluent stream which is monitored for polyvinyl alcohol concentration by differential refractometry. The solvent power of water was altered by varying its pH; hydrochloric

acid or sodium hydroxide were added to increase the hydrophilicity of the polyvinyl alcohol molecules because of the association of acid or base with the hydroxyl groups. The intrinsic viscosities of aqueous polyvinyl alcohol solutions of pH 2.5 and 11.5 were measured to investigate its effect on the solvent power of water. Table 4.9 shows the values of the intrinsic viscosities of Vinol 107 in water of pH 2.5 and 11.5, along with the corresponding values of α, which is related to the solvent power. The

TABLE 4.9

INTRINSIC VISCOSITY AND EXPANSION PARAMETER α FOR PVA IN DIFFERENT MEDIA

DESCRIPTION	INTRINSIC VISCOSITY dl/gm	α
In θ solvent (estimated)	0.3561	1.00
In water	0.4470	1.08
In water at pH 2.5	0.4498	1.08
In water at pH 11.5	0.4009	1.04

intrinsic viscosities in water of pH 2.5 and pure water were about the same, indicating little or no association of the hydrochloric acid with the hydroxyl groups; moreover, the intrinsic viscosity in water of pH 11.5 was lower than that in pure water. Thus the solvent power of water was not improved at acidic or basic pH values as compared with pure water. A part of the isotherm was also generated by desorption using water at pH 2.5. This showed no improvement on the extent of desorption that can be

achieved with pure water.

There is considerable disagreement as to the reversibility of polymer adsorption. It has been argued many times that the adsorption of polymers is irreversible because the polymer molecule forms multiple contacts with the surface, and the probability of the simultaneous detachment of all these contacts is small. It has also been argued (27) that the adsorption of polymers may be reversible, but requires long times and concentrations so low that they are impossible to detect. Each argument is true in a given case. Perhaps, the best solution to this problem is to consider polymer adsorption as irreversible for all practical purposes, at least under conditions of zero flow. Recently, it was demonstrated (99) that the application of hydrodynamic forces can dramatically increase the desorption of polymers, and complete desorption of the polymer may be possible at sufficiently high shear stresses.

4.2.10 Mechanism of Polymer Adsorption

The driving force for adsorption is the decrease in free energy of the system. Since the polymer loses some degree of freedom (and thus some entropy) on adsorption, the enthalpic contribution must be favorable for adsorption to occur. The enthalpic contribution to adsorption is postulated to arise from the formation of segment-surface and segment-segment contacts in the adsorbed layer. For the polystyrene-polyvinyl alcohol system, the polyvinyl

alcohol coil has a compact configuration in solution with relatively few segment-solvent contacts but establishes more segment-solvent contacts on adsorption. This concept is contrary to the earlier views on adsorption. The 0.499 value of the interaction parameter suggests strong interactions between the segments of the free polymer coil, and the high heats of adsorption suggest the formation of segment-solvent contacts in the adsorbed layer. The effect of curvature of the surface has been neglected in the formalism of any theory of adsorption. This work postulates that the curvature of the surface affects the configuration of the polymer coil in the adsorbed layer. To understand this effect, the configuration of polymer segments rather than the configuration of the entire coil must be considered. In contrast to the free polymer coil in solution, the segments of the adsorbed coil are present in at least two different states: the trains and the loops or the tails. The configuration of the segments in the trains are postulated to be affected by the curvature of the surface, which in turn determines the configuration of the rest of the coil. The polymer segments have maximum entropy in a random coil configuration and therefore tend to assume this configuration. When a polymer molecule in solution adsorbs on a curved or flat surface, its configuration changes from a three-dimensional random coil toward a two-dimensional coil, and the probability for the train segments to assume

a random configuration decreases because of the increasing loss of dimensionality, until the configuration becomes two-dimensional for a flat surface. Since the loss in entropy of the system must be minimized, segments from the trains are desorbed to form loops, and thicker films are formed with larger particles and on flat surfaces.

4.3 Conclusions

The use of high polyvinyl alcohol concentrations in adsorption experiments gives a rapid rise in the adsorption isotherm with increasing bulk concentration to a plateau in surface concentration, followed by a second rise in surface concentration. In contrast, adding excess polyvinyl alcohol to a colloidal sol is often postulated to give monolayer adsorption. The effect of increasing the polyvinyl alcohol molecular weight or decreasing its degree of hydrolysis is to increase the adsorption density and the adsorbed layer thickness. Good agreement between adsorption isotherms determined by adsorption and desorption experiments is observed with lower-molecular-weight polyvinyl alcohols. Desorption experiments give accurate values of the plateau concentrations, irrespective of the polyvinyl alcohol molecular weight, which is difficult to accomplish by adsorption experiments. The use of different particle size substrates gives similar adsorption isotherms with identical adsorption densities. The effect of particle size however, is manifested by an increase in the

thickness of the adsorbed layer with increasing particle size. The increase in adsorbed layer thickness results from changes in configuration of the adsorbed molecules on surfaces of different curvature. Heat measurement shows that the adsorption is a slow process, with plateau heat values attained only after several hours. The heats of adsorption are higher with polyvinyl alcohols of higher molecular weight and lower degree of lydrolysis, and are considerably higher than expected from mere segment-surface interactions. The higher heats result from increased segment-solvent interactions in the adsorbed layer. Heats of adsorption are lower on larger particles, and on flat surfaces. The plateau heat values are attained in shorter times with larger particles suggesting that the adsorption is a diffusion-controlled process governed by dispersion forces.

5. EFFECT OF ADSORBED POLYMER ON COLLOIDAL STABILITY

5.1 Introduction

The presence of polymer adsorbed at the interface plays an important role in the stabilization of colloidal sols. Electrostatic interactions between colloidal particles are well understood in terms of the DLVO (Derjaguin-Landau-Verwey-Overbeek) theory (39,43) developed in the early 1940's; however, an understanding of the steric interactions has been gained only in the past decade with the development of the HVO (Hesselink-Vrij-Overbeek) theory (53). Even today, there is no theory which can explain the more complicated case of combined electrostatic and steric stabilization.

Polystyrene latex particles prepared using persulfate ion initiator have chemically-bound strong-acid surface groups, which give these particles a net negative charge, and polyvinyl alcohol is a nonionic polymer. This polystyrene-polyvinyl alcohol system therefore represents a case of combined electrostatic and steric stabilization. One approach to evaluate this combined effect is to determine the potential energy of interaction between the particles in the presence and absence of the adsorbed polymer. Two basic experimental methods (61) have been used: i) measurement of the kinetics of coagulation or peptization; ii) measurement of the forces of interaction

as a function of the distance of separation between the particle surfaces.

Monodisperse polystyrene latex particles of 190nm and 400nm diameter were used in this investigation. The polyvinyl alcohol used was the fully-hydrolysed low-molecular-weight Vinol 107. The attractive forces between the bare and the PVA-covered particles were assumed to be identical. Electrolyte-stability measurements were made with the bare and PVA-covered polystyrene latex particles. Applied pressure during serum replacement was used to measure the repulsive forces between the bare and the PVA-covered particles.

5.2 Results and Discussion

5.2.1 Electrolyte Stability of Bare and PVA-Covered Polystyrene Latex Particles

Figure 5.1 shows that the variation of log W with log sodium chloride concentration for the bare and the Vinol 107-covered 190 and 400nm-size polystyrene latex particles was different for the different particle sizes, and the bare and PVA-covered particles. In all cases, the value of log W decreased with increasing log sodium chloride concentration to the intersection with the horizontal line of log W = 1. The descending line corresponds to the region of slow coagulation and the horizontal line, to the region of fast coagulation, and the electrolyte concentration at which these two lines intersect is defined as the critical

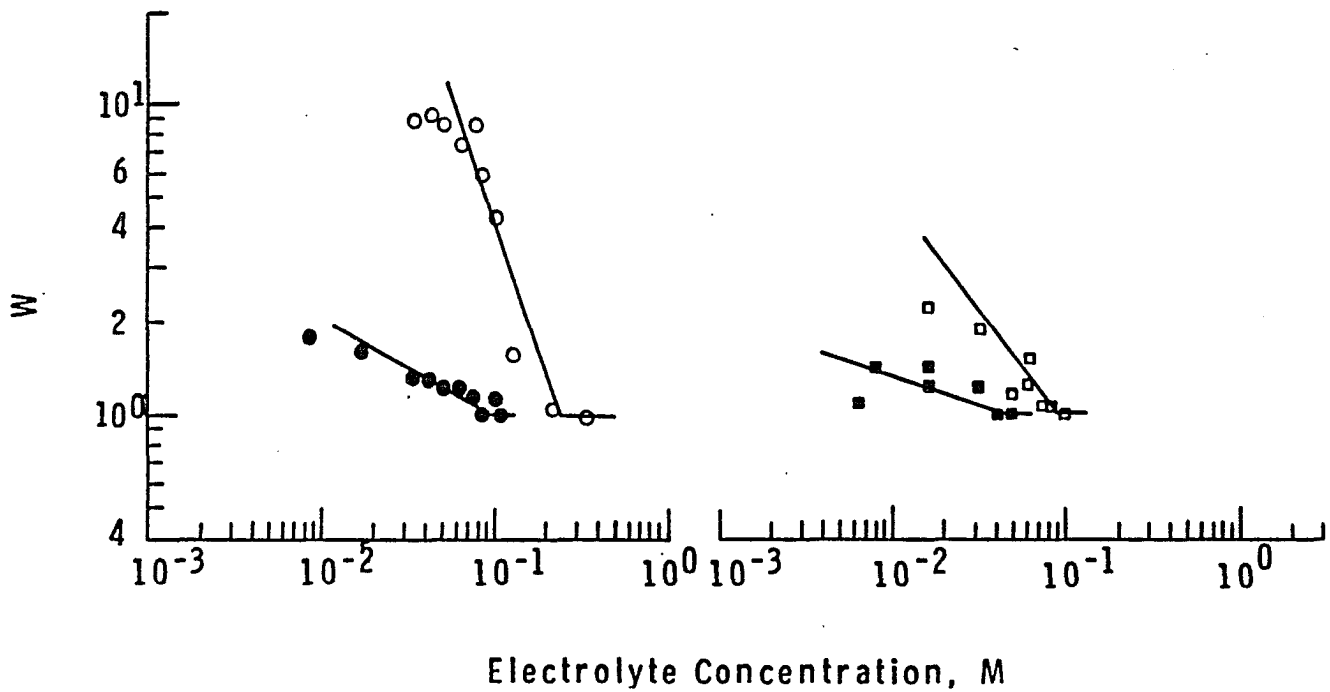

Figure 5.1 W versus electrolyte concentration (NaCl) for different-size particles: (o) 190nm particles; (□) 400nm particles; open points for bare particles and closed points for particles covered with Vinol 107 at saturation.

coagulation concentration (CCC). The slopes of the log W-log sodium chloride concentration lines were steeper for the bare particles than for the PVA-covered particles. Table 5.1 gives the CCC values and the slopes of the descending lines of the log W-log electrolyte concentration plots. As expected, the CCC of the 400nm-size particles was about 2.4 times smaller than that of the 190nm-size particles. The slope of the descending line was also about 2.5 times smaller for the 400nm-size particles than for the 190nm-size particles. According to Reerink and Overbeek (80), steeper slopes are expected for larger-size particles; however, this was not always observed experimentally. The intersection occurred at lower electrolyte

TABLE 5.1

CRITICAL COAGULATION/FLOCCULATION CONCENTRATION AND THE SLOPE OF LOG W VS LOG C PLOT

LATEX SAMPLE	CCC/CFC,mM	$-\frac{d\log W}{d\log(c)}$
190nm Bare Particles	225	1.69
190nm Covered Particles	98	0.23
400nm Bare Particles	95	0.66
400nm Covered Particles	40	0.22

concentrations for the PVA-covered particles than for the bare particles, which was unexpected; this was attributed to the flocculation of the PVA-covered particles in the secondary minimum as opposed to the coagulation of the

bare particles in the primary minimum of the potential energy diagram. The terms "flocculation" and "coagulation" are used to denote the respective reversibility or irreversibility of this association. For the PVA-covered particles, the descending lines of the PVA-covered particles corresponded to the region of slow flocculation and the horizontal lines, to that of fast flocculation; the presence of a strong nonionic steric barrier restricts the flocculation to the shallow secondary minimum. The electrolyte concentration at which these two lines intersect is defined as the critical flocculation concentration (CFC). Table 5.1 also gives the CFC values and the slopes of the descending lines. The CFC value of the 400nm-size particles was about one-half that of the 190nm-size particles; however, the slopes of the descending lines were identical. Comparison of the slopes of the descending lines for the bare and PVA-covered particles showed that the rate of slow flocculation of the PVA-covered particles was slower than that of slow coagulation of the bare particles.

These measurements are valid for the coagulation of the electrostatically stabilized bare polystyrene particles in the primary minimum. They are less valid for the coagulation of particles which are sterically stabilized with a nonionic polymer stabilizer, where the high steric barrier to coagulation is insensitive to electrolyte. Nonetheless,

such measurements have been used to determine the effect of nonionic stabilizers on the stability of colloidal sols by earlier workers (100,101), who found that the electrolyte concentration required for coagulation/flocculation increased with increasing concentration of adsorbed nonionic emulsifier. This result was attributed to the strong steric barrier arising from the adsorbed layer and the reduction in the attractive forces. It should be emphasized that the stabilizers used in these earlier studies were of low molecular weight, and the possibility of desorption on dilution during the experiments cannot be ruled out.

These measurements are probably more valid for the PVA-covered particles because of the absence of any desorption on dilution. The effect of electrolyte on the flocculation in the secondary minimum is unknown. The depth of the secondary minimum for these PVA-covered particles, calculated from the thickness of the adsorbed layer, and neglecting the effect of the adsorbed layer and the retardation forces, is of the order of 0.25-0.50 kT. Since the average kinetic energy of a particle is of the order of 1 kT, these particles should be stable indefinitely. This is the case for the PVA-covered particles in the absence of electrolyte; however, the addition of electrolyte could have affected the depth of the secondary minimum, so that this minimum was deeper for the 400nm-size particles than for the 190nm-size particles. This deeper secondary minimum

could explain the flocculation of the 400nm-size particles at lower electrolyte concentrations than for the 190nm-size particles.

5.2.2 Electrophoretic Mobility of Bare and PVA-Covered Polystyrene Latex Particles

Figure 5.2 shows the variation of electrophoretic mobility with sodium chloride concentration for the bare and the Vinol 107-covered polystyrene particles of 190nm and 400nm diameter. For the bare particles, the electrophoretic mobility remained constant up to a critical electrolyte concentration, then increased to a maximum and decreased sharply, and finally approached zero. The maximum in the electrophoretic mobility-electrolyte concentration curve for the bare particles was explained earlier (102) by the adsorption of chloride ions on the hydrophobic polystyrene latex particle surface. In contrast, for the PVA-covered particles, the electrophoretic mobility decreased with increasing electrolyte concentration until it approached zero at high electrolyte concentration. The adsorption of polymer moves the slipping or shear plane further out from the particle surface, and its distance from the surface becomes sensitive to the electrolyte concentration. It is interesting that the electrolyte concentration at which the electrophoretic mobility reached zero was close to the foregoing CCC/CFC values.

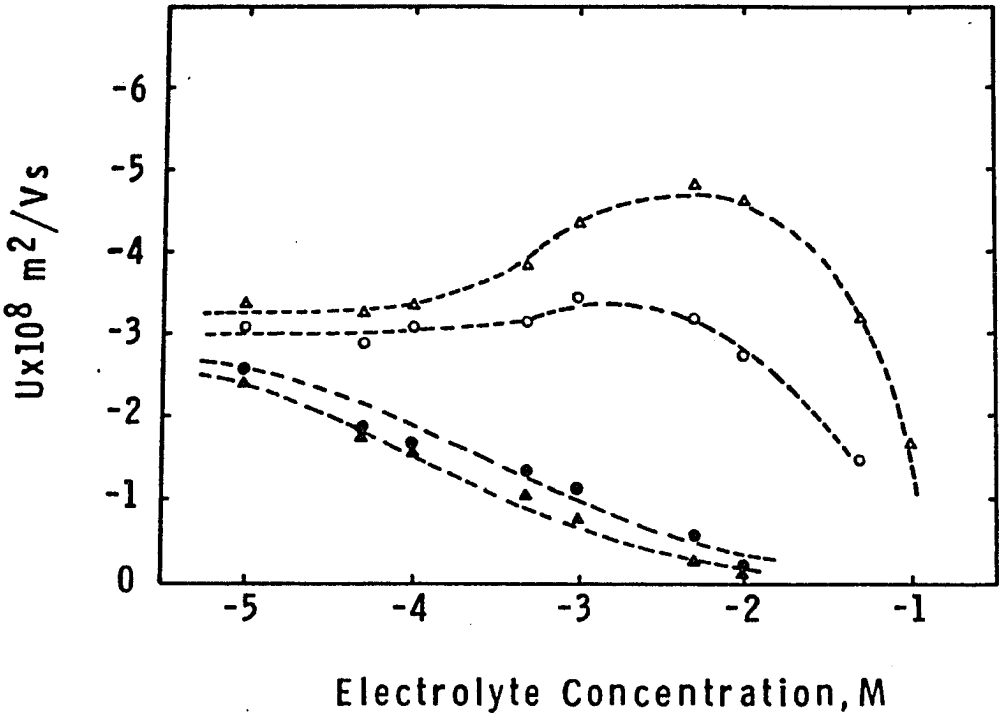

Figure 5.2 Electrophoretic mobility versus electrolyte concentration (NaCl) for different-size particles: (o) 190nm particles; (Δ) 400nm particles; open points for bare particles and closed points for particles covered with Vinol 107 at saturation.

5.2.3 Repulsive Forces Between Bare and PVA-Covered Polystyrene Latex Particles

Figure 5.3 shows the pressure-volume fraction curves for the bare and PVA-covered polystyrene particles of 190 and 400nm diameter. The differences between the curves for the two different-size particles were insignificant, but the differences between the bare and the PVA-covered particles were distinct. For the bare particles, the pressure increased gradually up to a volume fraction of about 0.44 and then increased sharply. For the PVA-covered particles, the steep rise in pressure occurred at a higher volume fraction (0.59). Table 5.2 shows the maximum volume fractions for the different samples and the distances of separation at these volume fractions calculated according to the relationship (103):

$$H = \left(1.81a/\phi^{1/3}\right) - 2a \qquad 5.1$$

where H is the distance of separation, a the particle diameter, and ϕ the volume fraction of the particles. The smallest distance of separation, which was achieved with the PVA-covered particles, was almost twice the thickness of the adsorbed layer. It was not possible to compress these particles further because further increases in nitrogen gas pressure resulted in gas leakage from the cell outlet. Removal of the sample from the cell showed that particles had formed a cake. Examination of this cake

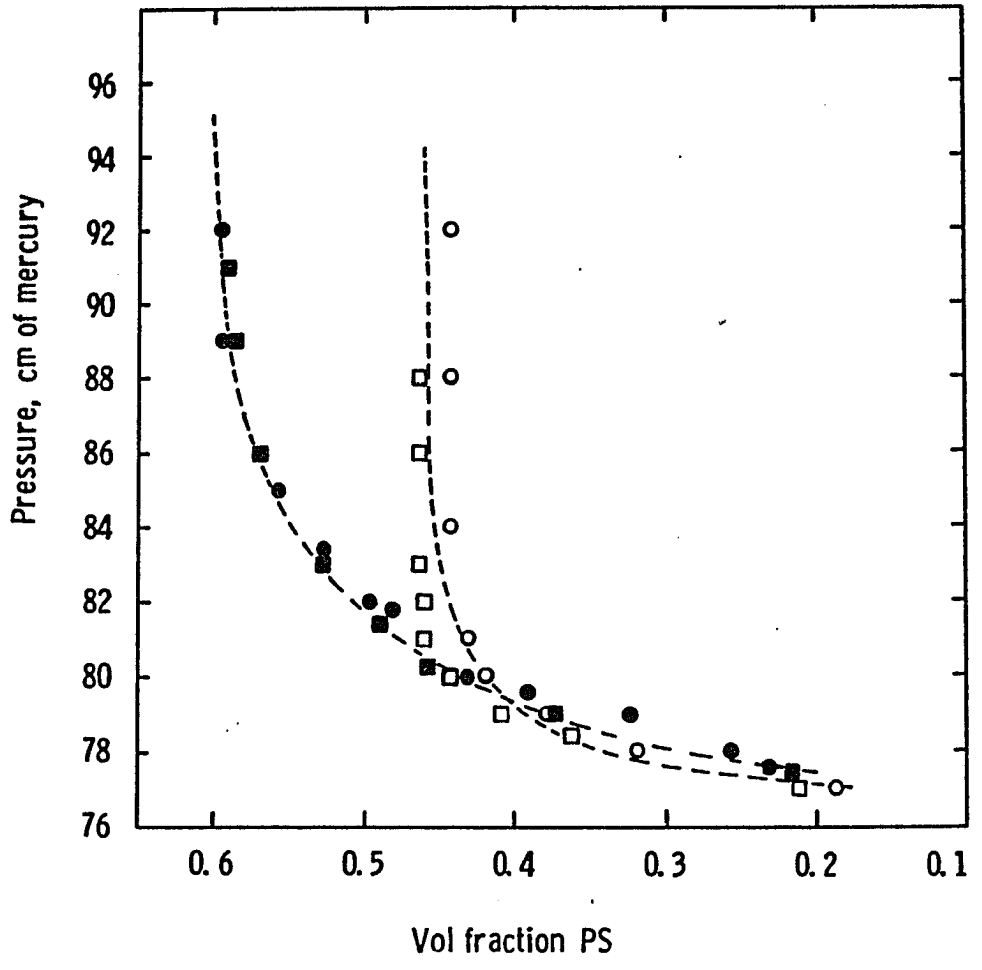

Figure 5.3 Pressure versus volume fraction polystyrene for different size particles: (o) 190nm particles; (□) 400nm particles; open points for bare particles and closed points for particles covered with Vinol 107 at saturation.

TABLE 5.2

MAXIMUM VOLUME FRACTION AND THE CLOSEST DISTANCE OF SEPARATION BETWEEN THE PARTICLES FOR THE PVA-PS SAMPLES

SAMPLE	MAX VOL FRACT	DISTANCE OF SEPARATION(nm)
PS 190nm	0.44	71.1
PS 400nm	0.46	135.2
PS 190-107	0.59	30.0
PS 400-107	0.58	68.2

by scanning electron microscopy (Figures 5.4-5.7) showed that the particles were packed in hexagonal close-packed arrays, crystalline structures with the latex particles as the primary units. To estimate the maximum repulsive forces requires that the primary repulsion maximum must be exceeded, which would lead to coagulation of the particles. Clearly, this did not occur with these samples. Also, it was not possible to calculate the repulsive forces from the applied pressures because the calculation requires an accurate value of the area of interaction, which is difficult to determine.

5.3 Conclusions

Electrolyte-stability measurements of bare and PVA-covered polystyrene particles showed that the rate of slow flocculation of the PVA-covered particles was slower than the rate of slow coagulation of the bare particles. This was attributed to flocculation of the PVA-covered

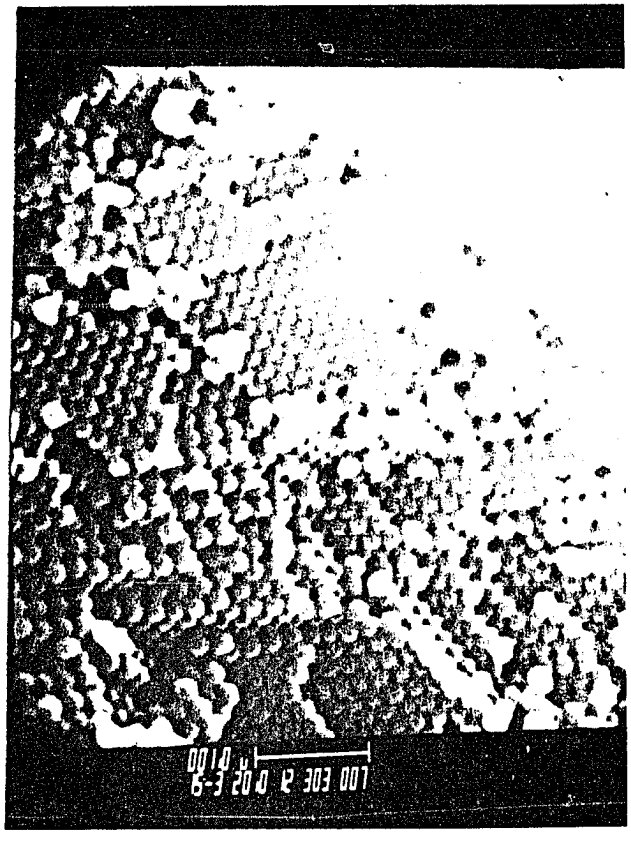

Figure 5.4 Scanning electron micrograph of compressed 190nm polystyrene latex cake.

Figure 5.5 Scanning electron micrograph of compressed Vinol 107-covered 190nm polystyrene latex cake.

Figure 5.6 Scanning electron micrograph of compressed 400nm polystyrene latex cake.

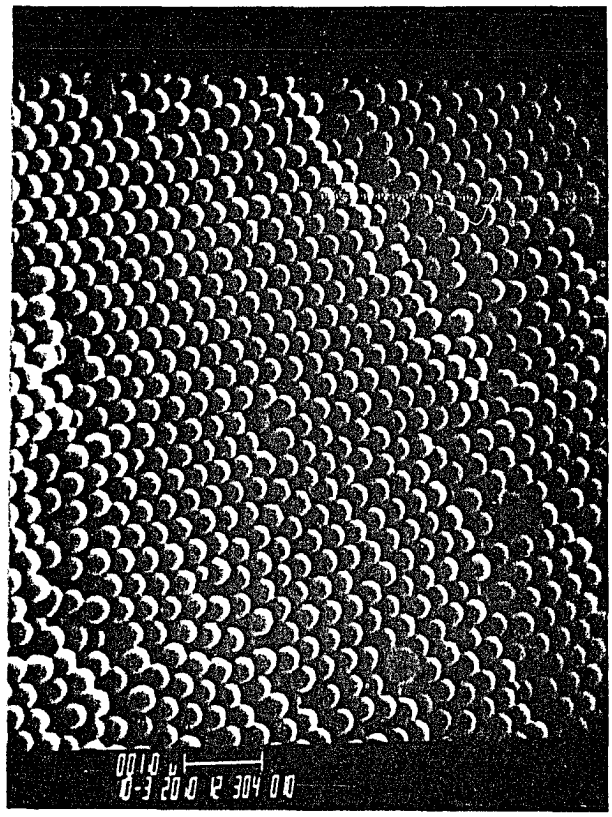

Figure 5.7 Scanning electron micrograph of compressed Vinol 107-covered 400nm polystyrene latex cake.

particles in the secondary minimum as compared with coagulation of the bare particles in the primary minimum. The PVA-covered particles flocculated at lower electrolyte concentrations than the bare particles, and the flocculation was reversible. Electrophoretic mobility measurements corroborated the electrolyte-stability measurements. The pressure-volume fraction curves for the bare and the PVA-covered particles showed a gradual increase in pressure at low volume fractions followed by a steep rise in pressure at volume fractions of 0.44 for the bare and 0.59 for the PVA-covered particles. At these volume fractions, the latex particles were packed into hexagonal close-packed arrays.

6. RECOMMENDATIONS FOR FUTURE WORK

Both the theoretical and experimental concepts of polymer adsorption should be developed further until a complete understanding of the process is gained. Although the theoretical aspects of polymer adsorption have received far more attention than the experimental aspects, no satisfactory explanation has been advanced for such complicated phenomena as desorption and configuration of the adsorbed molecules, and no theory has treated the effect on the various adsorption parameters of the surface curvature, which affects the configuration of the adsorbed molecules. Obviously, this is an important parameter for theoretical consideration.

With the development of sophisticated techniques such as pulse nuclear magnetic resonance spectroscopy and small-angle neutron scattering, it has become possible to determine the configuration of the adsorbed polymer molecules more exactly than before. These techniques should be used to study the effect of the curvature of the substrate surface on the various adsorption parameters. In this work, the effect of the particle size of the latex particle substrate was investigated systematically, but because of the nature of the system and the length of time involved, the experimental determination of the configuration of the adsorbed polymer molecules was not undertaken. It is sug-

gested that a different polymer adsorbate be used, which would help in the generalization of the results and the configuration examined. An outline of the various experiments that should be carried out is given below:

i) preparation of monodisperse deuterated polystyrene latex particles of different sizes (100nm-1000nm) to use the pulse NMR and small-angle neutron scattering techniques;

ii) determination of the adsorption isotherms by the adsorption and desorption serum replacement techniques;

iii) determination of the thickness of the adsorbed layer;

iv) determination of the heats of adsorption by microcalorimetry;

v) determination of the polymer bound fraction by pulse NMR spectroscopy;

vi) determination of the segmental density distribution by small-angle neutron scattering.

A good candidate for the polymer adsorbate would be polyvinyl pyrolidone of moderate molecular weight because of its importance as a stabilizer and its use in the preparation of large-particle-size monodisperse latexes in microgravity.

REFERENCES

1. Eirich, F.R., J. Colloid Interface Sci., 1977, 58, 423.

2. Vincent, B., and Whittington, S.F., Surface Colloid Sci., ed. E. Matijevic, Plenum Press, New York, 1982, 12, 1.

3. Takahashi, A., and Kawaguchi, M., Adv. Polym. Sci., 1982, 46, 1.

4. Tadros, Th.F., "The Effect of Polymers on Dispersion Properties," ed. Th.F. Tadros, Academic Press, London, 1982, 1.

5. Fleer, G.J., and Lyklema, J., "Adsorption from Solution at the Solid/Liquid Interface," ed. G.D. Parfitt, Academic Press, New York, 1983, 153.

6. Vincent, B., "Polymer Adsorption and Dispersion Stability", ed. E.D. Goddard and B. Vincent, ACS Symp. Ser 240, 1984, 1.

7. Jenckel, E., and Rumbach, R., Z. Electrochem., 1951, 55, 612.

8. Killmann, E., Polymer, 1976, 17, 864.

9. Fontana, B.J., and Thomas, J.R., J. Phys. Chem., 1961, 65, 480.

10. Killmann, E., Eisenlauer, J., and Korn, M., J. Polym. Sci., 1977, C61, 413.

11. Barnett, K., Cosgrove, T., Crowley, T.L., Tadros, Th.F., and Vincent, B., "The Effect of Polymers on Dispersion Properties," ed. Th.F. Tadros, Academic Press, New York 1982, 199.

12. Frisch, H.L., Simha, R., and Eirich, F.R., J. Chem. Phys., 1953, 21, 365.

13. Simha, R., and Eirich, F.R., J. Phys. Chem., 1953, 57, 584.

14. Frisch, H.L., and Simha, R., J. Phys. Chem., 1954, 58, 507.

15. Frisch, H.L., J. Phys. Chem., 1955, 59, 633.

16. Frisch, H.L., and Simha, R., J. Chem. Phys., 1957, 27, 702.

17. Silberberg, A., J. Phys. Chem., 1962, 66, 1872.

18. Silberberg, A., J. Phys. Chem., 1962, 66, 1884.

19. Silberberg, A., J. Phys. Chem., 1967, 46, 1105.

20. Silberberg, A., J. Phys. Chem., 1968, 48, 2835.

21. Silberberg, A., J. Colloid Interface Sci., 1972, 38, 217.

22. Hoeve, C.A.J., J. Chem. Phys., 1965, 42, 2558.

23. Hoeve, C.A.J., J. Chem. Phys., 1965, 43, 3007.

24. Hoeve, C.A.J., J. Chem. Phys., 1966, 44, 1505.

25. Hoeve, C.A.J., J. Polym. Sci., 1970, C30, 361.

26. Hoeve, C.A.J., J. Polym. Sci., 1971, C34, 1.

27. Scheutjens, J.M.H.M., and Fleer, G.J., J. Phys. Chem., 1979, 83, 1619.

28. Scheutjens, J.M.H.M., and Fleer, G.J., J. Phys. Chem., 1980, 84, 178.

29. Lipatov. Yu.S., and Sergeeva, L.M., "Adsorption of Polymers," English transl., Keter Publ. House, 1974, 31.

30. Heller, W., and Pugh, T.L., J. Chem. Phys., 1954, 22, 1778.

31. Hamaker, H.C., Physics, 1937, 4, 1058.

32. Lifshitz, E.M., Sov. Phys., 1956, JETP (Engl. Transl.), 2, 73.

33. Vold, M.J., J. Colloid Sci., 1961, 16, 1.

34. Vincent, B., J. Colloid Interface Sci., 1973, 42, 270.

35. Gouy, G., J. Phys., 1910, 9, 457.

36. Chapman, D.L., Phil Mag., 1913, 25, 475.

37. Stern, O.Z., Z. Electrochem., 1924, 30, 508.

38. Grahame, D.C.Z., Z. Electrochem., 1958, 62, 264.

39. Verwey, E.J., and Overbeek, J.Th.G., "Theory of the Stability of Lyophobic Colloids," Elsevier, Amsterdam, 1948.

40. Derjaguin, B.V., Acta Phys. Chim. USSR, 1939, 10, 333.

41. Derjaguin, B.V., Kolloidn, Zh., 1940, 6, 291.

42. Derjaguin, B.V., Kolloidn. Zh., 1941, 7, 285.

43. Derjaguin, B.V., and Landau, L.D., Acta Phys. Chim. USSR, 1941, 14, 633.

44. Brooks, D.E., J. Colloid Interface Sci., 1973, 43, 687.

45. Mackor, E.L., J. Colloid Sci., 1951, 6, 492.

46. Mackor, E.L., and Van der Waals, J.H., J. Colloid Sci., 1952, 7, 535.

47. Clayfield, E.J., and Lumb, E.C., Disc. Faraday Soc., 1966, 42, 314.

48. Clayfield, E.J., and Lumb, E.C., J. Colloid Sci., 1966, 22, 269.

49. Clayfield, E.J., and Lumb, E.C., J. Colloid Sci., 1966, 22, 285.

50. Clayfield, E.J., and Lumb, E.C., Macromolecules, 1968, 1, 133.

51. Fisher, E.W., Kolloid-Z., 1958, 160, 120.

52. Meier, D.J., J. Phys. Chem., 1967, 71, 1861.

53. Hesselink, F.Th., Vrij, A., and Overbeek, J.Th.G., J. Phys. Chem., 1971, 75, 2094.

54. Hesselink, F.Th., J. Phys. Chem., 1969, 73, 3488.

55. Hesselink, F.Th., J. Phys. Chem., 1971, 75, 65.

56. Evans, R., and Napper, D.H., Kolloid Z.Z. Polym., 1973, 251, 329.

57. Napper, D.H., and Hunter, R.J., Surface Chem. Colloid, ed. M. Kerker, 1972, 1, 241.

58. Roberts, A.D., and Tabor, D., Nature, 1968, 219, 1122.

59. Roberts, A.D., and Tabor, D., Wear, 1968, 11, 163.

60. Barclay, L., and Ottewill, R.H., Spec. Disc. Faraday Soc., 1970, 1, 169.

61. Barclay, L., Harrington, A., and Ottewill, R.H., Kolloid Z.Z. Polym., 1972, 250, 655.

62. El-Aasser, M.S., and Robertson, A.A., J. Colloid and Interface Sci., 1971, 36, 86.

63. El-Aasser, M.S., and Robertson, A.A., Kolloid Z.Z. Polym., 1973, 250, 6555.

64. Doroszkowski, A., and Lambourne, R., J. Polym. Sci., 1971, C34, 253.

65. Doroszkowski, A., and Lambourne, R., J. Colloid Interface Sci., 1973, 43, 97.

66. Andrew, D.M., Marev, E.D., and Hayden, D.A., Spec. Disc. Faraday Soc., 1970, 1, 46.

67. Homola, A., and Robertson, A.A., J. Colloid Interface Sci., 1976, 54, 286.

68. Cain, F.W., Ottewill, R.H., and Smitham, J.B., Faraday Disc. Chem. Soc., 1978, 65, 33.

68a. Osmond, D.W.J., and Waite, F.A., "Dispersion Polymerization in Organic Media", ed. K.E.J. Barrett, John Wiley & Sons, 1975.

69. Vanderhoff, J.W., van den Hul, H.J., Tausk, R.J.M., and Overbeek, J.Th.G., "Clean Surfaces: Their Preparation and Characterization for Interfacial Studies," ed. G. Goldfinger, Marcel Dekker, New York, 1970, 15.

70. van den Hul, H.J., and Vanderhoff, J.W., Brit. Polym. J., 1970, 2, 121.

71. Vanderhoff, J.W., and van den Hul, H.J., J. Colloid Interface Sci., 1968, 28, 336.

72. Burchard, W., Makromol Chem., 1961, 50, 20.

73. Stockmayer, W.H., and Fixman, M., J. Polym. Sci., 1963, C1, 137.

74. Koopal, L.K., Ph.D. Thesis, Meded. Landbouwhogeschool, Wageningen, 1978, 78-12.

75. Ahmed, S.M., El-Aasser, M.S., Micale, F.J., Poehlein, G.W., and Vanderhoff, J.W., "Polymer Colloids," ed. R.M. Fitch, 1980, 265.

76. Fleer, G.J., Ph.D. Thesis, Meded. Landbouwhogeschool, Wageningen, 1971, 71-20.

77. Brown, J.C., Pusey, P.N., and Dietz, R., J. Chem. Phys., 1975, 62, 1136.

78. Berne, B.J., and Pecora, R., "Dynamic Light Scattering," John Wiley & Sons, New York, 1976.

79. Derderian, E.J., and MacRury, T.B., J. Dispersion Sci. Technol., 1981, 2, 345.

80. Reerink, H., and Overbeek, J.Th.G., Faraday Soc. Disc., 1954, 18, 74.

81. Chem. Marketing Reporter, Dec. 8, 1978, 9, 214.

82. Oblonkova, E.S., Rogovina, L.Z., Dinitrieva, N.A., Belavtseva, E.M., and Slonimskii, G.L., Kolloidn. Zh. (Engl. Transl.), 1974, 36, 284.

83. Matsumoto, M., and Ohyanagi, Y., J. Polym. Sci., 1958, 122, 31, 226.

84. Beresniewics, A., J. Poly. Sci., 1959, 35, 321.

85. Beresniewics, A., J. Poly. Sci., 1959, 39, 63.

86. Lankveld, J.M.G., Ph.D. Thesis, Meded. Landbouwhogeschool, Wageningen, 1970, 70-21.

87. Pritchard, J.D., "Polyvinyl Alcohol, Basic Properties and Uses", Gordon and Breach, London, 1970.

88. Garvey, M.J., Ph.D. Thesis, University of Bristol, 1974.

89. Flory, P.J. and Fox, T.G., J. Am. Chem. Soc., 1951, 73, 1904.

90. Tanford, C.H., "Physical Chemistry of Macromolecules," John Wiley & Sons, New York, 1961.

91. Kurata, M., and Stockmayer, W.H., Fortschr. Hochpolym. Forsch., 1963, 3, 196.

92. Cohen-Staurt, M.A., Scheutjens, J.M.H.M., and Fleer, G.J., J. Poly. Sci., Polym. Phys. Ed., 1980, 18, 559.

93. Clark, A.T., and Lal, M., "The Effect of Polymers on Dispersion Properties," ed. Th.F. Tadros, 1982, 169.

94. Boomgaard, Th.V., King, T.A., Tadros, Th.F., Tang, H., and Vincent, B., J. Colloid Interface Sci., 1978, 66, 68.

95. Ahmed, M.S., El-Aàsser, M.S., and Vanderhoff, J.W., paper presented at the 56th Colloid and Surface Sci. Symp., Blacksburg VA, June 1982.

96. Killmann, E., Strasser, H.J., Winter, K., Int. Kongr. Grenzflachenaktive Stoffe, Zurich, 1972, III, 221.

97. Hagiopal, C., Georgecu, M., Deleanu, Th., and Dimonie, V., Colloid Polym. Sci., 1979, 257, 1196.

98. Saito, S., J. Polym. Sci., 1969, 7, 1789.

99. Fuller, G.G., and Lee, J., "Polymer Adsorption and Dispersion Stability," ed. E.D. Gooddard and B. Vincent, ACS Symp. Ser., 1984, 240, 67.

100. Mathai, K.G., and Ottewill, R.H., Trans. Faraday Soc., 1966, 62, 759.

101. Ottewill, R.H., and Walker, T., Kolloid Z. Z. Polym., 1968, 227, 108.

102. Ma, C.M., Micale, F.J., El-Aasser, M.S., and Vanderhoff, J.W., "Emulsion Polymers and Emulsion Polymerization," ed. D.R. Bassett and A.E. Hamielic, ACS Symp. Ser. 1981, 165, 251.

103. Albers, W., and Overbeek, J.Th.G., J. Colloid Sci., 1959, 14, 510.

APPENDIX A

CALCULATION OF INTERACTION PARAMETER 'χ'

$$B = \beta M_s^{-2} = v^2 (1-2\chi)(V_1 N_A)^{-1}$$

B from Burchard-Stockmayer-Fixman Relationship (eq. 2.6)

v = specific volume of polymer (PVA) = 0.77 $cm^3 g^{-1}$

V_1 = molar volume of solvent (Water) = $18 cm^3\ mol^{-1}$

N_A = Avogadro's number = $6.02 \times 10^{23}\ mol^{-1}$

APPENDIX B

CALCULATION OF HEAT OF ADSORPTION

POR = the print out reading

For 15 minutes run:

$$J/m^2 = \frac{\text{POR at 15 minutes - POR at 5 minutes}}{\text{Total Surface Area}}$$

For 180 minutes run:

$$J/m^2 = \frac{\text{POR at 180 minutes - POR at 5 minutes}}{\text{Total Surface Area}}$$

APPENDIX C

CALCULATION OF THE DEPTH OF THE SECONDARY MINIMUM

Van der Waals attraction potential ΔG_A (neglecting the retardation and Vold effects)

$$[\Delta G_A/kT] = - (A/12kT)\ H\ (x)$$

where

$$H(x) = \frac{1}{x^2+2x} + \frac{1}{x^2+2x+1} + 2\ell n \frac{x^2+2x}{x^2+2x+1}$$

$x = Ho/2R$

Ho = minimum distance of separation $\sim 2\delta$

R = radius of the particle

VITA

Maqsood Syed Ahmed was born July 25, 1954 in Hyderabad City - India, son of Kursheed Siddiqua and Syed Mohammed. He received his school education at Madarsa-i-Aliya, Hyderabad, India. He was awarded the state merit scholarship for his performance during high school.

Mr. Ahmed entered Nizam College in Hyderabad, India, where he graduated in 1975 with a B.Sc in chemistry. He pursued his studies in chemistry at Osmania University, Hyderabad, India, where he received his M.Sc degree in Chemistry in 1977.

Mr. Ahmed came to Lehigh University in 1979 for graduate studies in Polymer Science and Engineering. He was a teaching assistant in Chemistry Department for a semester after which he joined the Emulsion Polymers Institute as a research assistant. He received his M.S. in Polymer Science and Engineering in 1981. Upon graduation from Lehigh University, Mr. Ahmed has accepted a position as a research scientist with Rohm and Haas Company.